UNIVERSITÀ
DEGLI STUDI
DI PADOVA

Head Office: Università degli Studi di Padova

Department of Cardio-Thoraco-Vascular Sciences and Public Health

Ph.D. COURSE IN: Translational Specialistic Medicine “G.B. Morgagni”
CURRICULUM: Neuroscience
SERIES 35°

Ophthalmological involvement in wild-type, hereditary transthyretin and light chain amyloidosis: a multimodal imaging study

Coordinator: Prof.ssa Annalisa Angelini
Supervisor: Prof.ssa Chiara Briani

Ph.D. student : Luisa Frizziero

INDEX

1 ABSTRACT

Background: The prevalence and clinical relevance of transthyretin (ATTR) amyloidosis has been growing continuously in recent years, particularly for the increasing knowledge of the wild type form (ATTRwt). Ophthalmological abnormalities have been reported in hereditary transthyretin (ATTRv, v for variant) amyloidosis but only anecdotally in ATTRwt amyloidosis. The present study aimed at investigating the ophthalmologic involvement in ATTRwt, also compared with ATTRv and light chain (AL) amyloidosis and the possible role of non-invasive imaging modalities in the ocular assessment of these patients.

Methods: This was a cross-sectional, non-interventional study. Patients affected by ATTR or AL amyloidosis referred to the Department of Neuroscience of the University of Padua were recruited. Patients' records were reviewed for assessing the systemic involvement of amyloidosis, the presence of genetic mutations and detecting other systemic comorbidities, such as diabetes, to be taken into account as potential confounders in the analysis. An age-matched control group of healthy subjects was also studied. All the patients underwent a complete eye examination, including best-corrected visual acuity assessment (BCVA), anterior segment examination, evaluating in particular the presence of any deposits and alterations involving the iris and the lens, intraocular pressure, fundus examination, optical coherence tomography (OCT, for the evaluation of the retinal layers) and OCT angiography (for the non-invasive evaluation of the retinal vasculature) and *in vivo* corneal confocal microscopy (CCM, for the non-invasive study of corneal structures, in particular of the corneal nerve plexuses).

Results: Thirty-five patients were enrolled: 17 ATTRwt, 9 ATTRv, 2 pre-symptomatic carriers and 7 AL. The mean age was 70.1 $\pm$ 11 years. In the control group, 49 healthy subjects with a mean age of 66.2 $\pm$ 10.2 years were enrolled (p=0.0964). Visual acuity was significantly reduced in all patients (and particularly those with ATTRwt amyloidosis) compared to controls (p=0.0001). Seven patients were affected by glaucoma, two of

them (ATTRwt) newly diagnosed; one of them presented a picture of pseudoexfoliatio lentis. Fifty percent of ATTRwt patients had cataract and 38% had already undergone cataract surgery. Eighteen patients presented with abnormal findings of the retinal pigment epithelium at OCT, with advanced macular degeneration in three patients. Six patients had alterations of the vitreomacular interface. Vitreous opacities were identified in 7 patients. Corneal deposits were identified in 6 ATTRwt patients. CCM showed corneal deposits in 16 patients, reduced nerve fiber length ($p=0.0230$) and tortuous stromal nerves ($p=0.0094$) compared to controls. OCT showed a reduction in macular volume and in the peripapillary nerve fiber layer thickness. OCT angiography found a significant impairment of the retinal vascularization, both of radial peripapillary capillary plexus and macular vascular plexuses ($p<0.05$), compared to controls.

Conclusions: Ophthalmologic manifestations are common in amyloidosis patients, particularly in ATTRwt amyloidosis, potentially leading to a significant reduction in visual acuity and quality of life. Although age may have influenced the results, the prevalence and severity of the pathological findings suggests a relevant pathogenic role of amyloid in their development. Therefore, it is important to emphasize the importance of multidisciplinary management and thorough ophthalmological assessment, follow-up and timely treatment, when necessary. Moreover, non-invasive imaging modalities, such as CCM and OCT may allow the identification and follow-up of signs of damage at the level of specific structures, such as small nerve fibers and small vessels, more difficult to analyze at a systemic level.

2 INTRODUCTION

2.1 THE EYE

The eye is the primary organ of vision. However, it is also now considered a mirror of the complex pathophysiological phenomena occurring in the whole body, both in physiological and pathological conditions. This is particularly true for the central nervous system, since the retina and optic nerve are outgrowths from the brain.

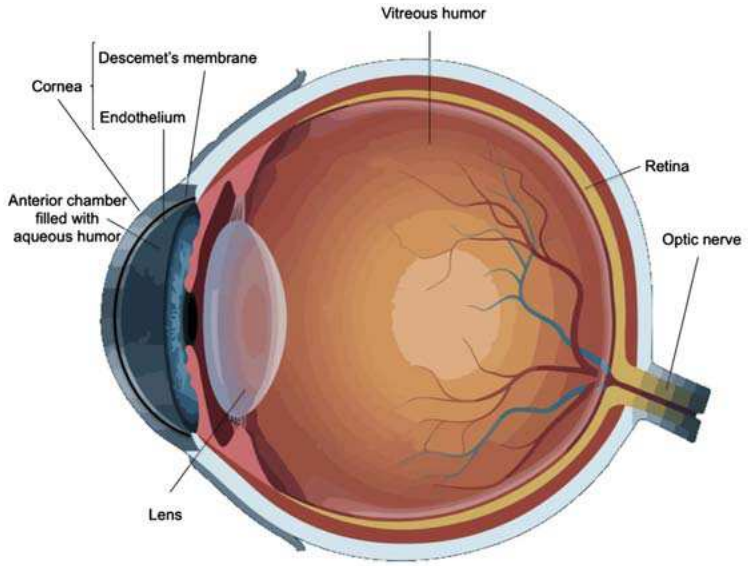

Figure 1. Diagram of the eye structure.[1]

2.1.1 Anatomy

Three concentric layers constitute the eye: the outer fibrous layer is composed of the cornea, the sclera and the lamina cribrosa; the middle vascular layer (“uveal tract”) in composed of the iris, the ciliary body and the choroid; The inner nervous layer is represented by the retinal pigment epithelium (RPE) and the neuroepithelium.

The *cornea* constitutes the anterior one-sixth of the fibrous layer, is transparent and has five layers antero-posteriorly:

- The epithelium is a stratified squamous type of epithelium with five to six cell layers with regular arrangement.

- The Bowman's layer is a homogeneous sheet of modified stroma.
- The stroma constitutes approximately 90% of total corneal thickness and is formed by lamellae of collagen, cells and ground substance.
- The Descemet's membrane is the basement membrane of the endothelium.
- The endothelium is a single layer of cells lining the inner surface of Descemet's membrane.

The cornea is highly innervated. In particular, corneal nerves arise from the ophthalmic branch of the trigeminal nerve, that contains myelinated A-fibers that lose their myelin sheath within 1 mm of the limbus to guarantee corneal transparency, and unmyelinated C fibers. These fibers enter in the middle stroma and then track anteriorly reaching and penetrating the Bowman's layer, where they spread in a network of fibers running parallel to the cornea surface forming the sub-basal plexus.[2] (Figure 1)

The *sclera* consists of irregular lamellae of collagen fibers and forms the posterior five-sixths of the fibrous layers. The junction with the cornea is the limbus, where the epithelium of the outer surface of the cornea becomes continuous with that of the conjunctiva, a thin, loose transparent non-keratinising mucous membrane that covers the anterior part of the sclera.

The *iris* is a muscular structure constituting the most anterior part of the uvea, perforated centrally by the pupil. Contraction of the iris sphincter muscle constricts the pupil, while contraction of the dilator pupillae muscle dilates the pupil.

The *ciliary body* is part of the uveal tissue and is attached anteriorly to the iris and the scleral spur; posteriorly it is continuous with the choroid.

The *choroid* consists of:

- The Bruch's membrane, located on the external surface of the RPE. It consists of the basement membrane of RPE cells and choriocapillaris. Between the two layers of basement membrane are the elastic and collagenous layers. Small localized thickenings of Bruch's membrane (which increase with age) are called drusen.

- The choriocapillaris, a network of capillaries supplying the RPE and outer retina.
- Layer of larger choroidal vessels external to the choriocapillaris.
- Suprachoroidal lamina.[3]

The *RPE* is a monolayer of cells linked to each other with tight junctions that form the external blood-eye barrier of the retina. RPE is important to maintain many functions of the retina including phagocytosis of the outer segment of photoreceptor cells, ion homeostasis, and the visual cycle transforming all-trans-retinol into 11-cis-retinal. 11-cisretinal is transported from the RPE to the photoreceptors through the interphotoreceptor matrix (IPM), where it binds to the opsin protein to form the visual pigment. Absorption of a photon of light catalyzes the isomerization of 11-cis-retinal to all-trans-retinal and results in its release. The isomerization triggers a cascade of events leading to the generation of an electrical visual signal. Once released, all-trans-retinal is converted to all-trans-retinol, which can be transported across the IPM to the RPE to complete the visual cycle. The source of all-trans-retinol in the RPE is ultimately the liver which secretes retinol bound to the transthyretin-retinol bind protein (TTR-RBP) complex. In RPE, free retinol uptake seems to be mediated by STRA6, a RBP cell membrane receptor which is highly expressed in the basolateral side of these cells.[4]

The *neuroepithelium* is made of multiple layers of cells distributed in a precisely manner, from the RPE to the vitreous:

- The photoreceptor layer, mainly composed by the outer segments of the photoreceptors: the cones, responsible for distinct and color vision, located above all in the macular region and in the fovea and the rods which are mainly located in the peripheral region, and responsible for scotopic vision. The photoreceptors represent the first neuron of the optic pathway.
- The outer limiting membrane (OLM), the site of the intercellular junctions between Müller cells and photoreceptor cells.

- The outer nuclear layer (ONL), mainly formed by photoreceptor nuclei.
- The outer plexiform layer (OPL), characterized by the synapses between photoreceptors and bipolar and horizontal cells.
- The inner nuclear layer (INL), which contains the nuclei of bipolar cells, the second neurons of the optic pathway, horizontal cells, amacrine cells and Müller cells.
- The inner plexiform layer (IPL), characterized by the synapses between bipolar cells, ganglion cells and amacrine cells.
- The ganglion cell layer (GCL), the site of ganglion cells nuclei, which represent the third neurons of the optic pathway.
- The retinal nerve fiber layer (RNFL), which represents the axons of the ganglion cells that converge in the optic nerve.
- The inner limiting membrane (ILM), formed by the terminal expansions of the Muller cells represents the border between the retina and the vitreous body.

From a topographical point of view, we may visualize:

- The posterior pole, including the macula and the optic nerve head, is included within the temporal vascular arcades.
- The optic nerve head represents the point of convergence of the nerve fibers, which correspond to the axons of the ganglion cells of the retina and forms the optic nerve.
- The macula has an approximate diameter of 5-6 mm, corresponding to the central 15-20 degrees of the visual field, is located temporally with respect to the optic disc and includes the fovea, the central excavation of the retina measuring about 1.5 mm in diameter, similar to that of the optic disc. (Figure 2)

Figure 2: Ultra-widefield color fundus photo of a healthy right eye, obtained using Clarus™ 500 fundus camera (Zeiss, Oberkochen, Germany) showing the posterior pole (circle), including the macula, the optic nerve head nasally to the macula and the periphery (beyond the vascular arcades).

Clinically, we can consider two segments: the anterior segment, from (and including) the lens forward and the posterior segment, including all structures posterior to the lens.

We can also recognize three compartments of the eye: the anterior chamber is the space between the cornea and the iris diaphragm and contains the aqueous humor, a watery, optically clear solution of water and electrolytes similar to tissue fluids except that aqueous humor has a low protein content normally. The posterior chamber is the triangular space between the iris anteriorly, the lens and zonule posteriorly, and the ciliary body while the vitreous chamber is the space behind the lens and zonule and contain the vitreous humor – a transparent gel consisting of a three-dimensional network of collagen fibers with the interspaces filled with polymerized hyaluronic acid molecules and water. It fills the space between the posterior surface of the lens, ciliary body and retina.[3] (Figure 1)

The vascularization of the eye derives from the carotid artery through the ophthalmic artery, from which three main vascular branches derive: the posterior ciliary arteries irrorating the anterior part of the optic nerve and the choroid and the muscular arteries for the extraocular muscles, both converge at the anterior segment of the eye. Finally, the retina artery creates the terminal vascularization of the retina. The central retinal artery, enters the eye through the optic disc, forming the four main vascular arcades, which remain on the surface of the retina and divide into smaller arteries and arterioles, then proceeding towards the deeper layers where only capillaries are present. We may therefore distinguish the superficial vascular plexus (SVP) located mainly in GCL and RNFL; the intermediate capillary plexus (ICP) located in the innermost part of the INL, and the deep capillary plexus (DCP) located in the outermost part of the INL and constituted only by capillaries. A fourth capillary network has also been identified, namely the radial peripapillary capillary plexus (RPCP), located in the nerve fiber layer and better represented in the peripapillary area with a typical anatomical organization, as the capillaries branch out parallel to the course of the ganglion cells axons with a radial arrangement, as opposed to the other capillary plexi in which the capillaries have a lobule arrangement, without a precise orientation. (Figure 3)

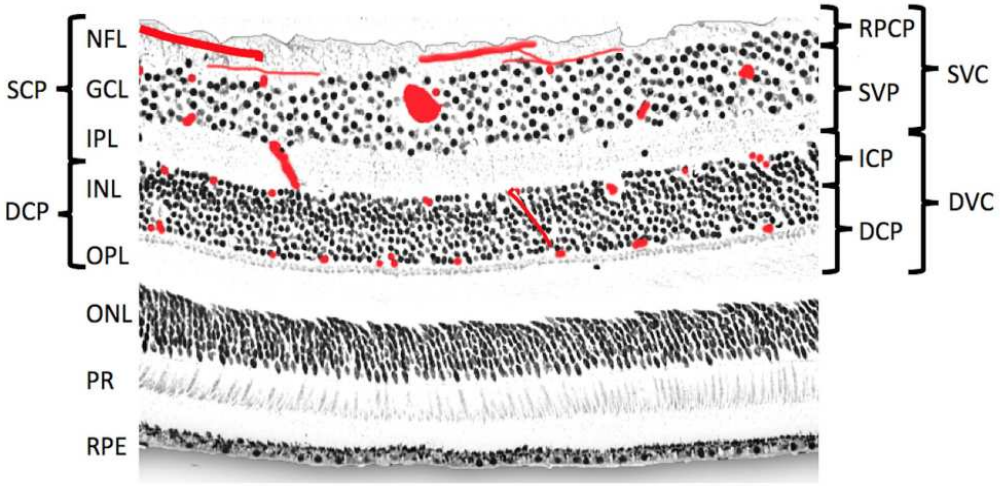

Current OCTA Nomenclature	Anatomic Layers	Proposed OCTA Nomenclature	
SCP	NFL	RPCP	SVC
	GCL	SVP	
	IPL		
DCP	INL	ICP	DVC
	OPL	DCP	

Figure 3: Anatomic localization of vascular plexuses in the human retina in the macula. NFL = nerve fiber layer, GCL = ganglion cell layer, IPL = inner plexiform layer, INL = inner nuclear layer, OPL = outer plexiform layer plus Henle's fiber layer, ONL = outer nuclear layer, PR = photoreceptor layers, RPE = retinal pigment epithelium, OCTA = optical coherence tomography angiography, RPCP = radial peripapillary capillary plexus, SVP = superficial vascular plexus, ICP = intermediate capillary plexus, DCP = deep capillary plexus.[5]

2.1.2 Diagnostic modalities

In recent years a huge technological evolution has involved the ophthalmological field, with particular regard to the diagnostic imaging modalities. Standard imaging modalities for imaging the posterior segment of the eye, include retinography and angiography. The first one provides a color fundus photo of the retina with a variable field of view, recently reaching 200°, thanks to the application of new light emission technologies.[6] (Figure 2) The second one uses the fluorescence of fluorescein and green indocyanine, which are injected into the systemic circulation, to visualize, in a dynamic way the retinal and choroidal vessels, respectively. It has the advantage to provide a dynamic information, although requiring the injection of intravenous dyes.

More recently, optical coherence tomography (OCT) has been introduced. OCT is a non-invasive imaging technique which uses light waves to take cross-section images of the retina and the choroid. It provides a layer by layer visualization of the chorioretina, also allowing an automatic segmentation of each layer. Therefore, it may produce quantitative information on the retinal and single layers thickness, in different location of the retina surface, including the macula and the peripapillary area. Moreover, it allows the visualization of the morphological changes involving the neuroepithelium, the RPE and the choroid.[7] (Figure 4)

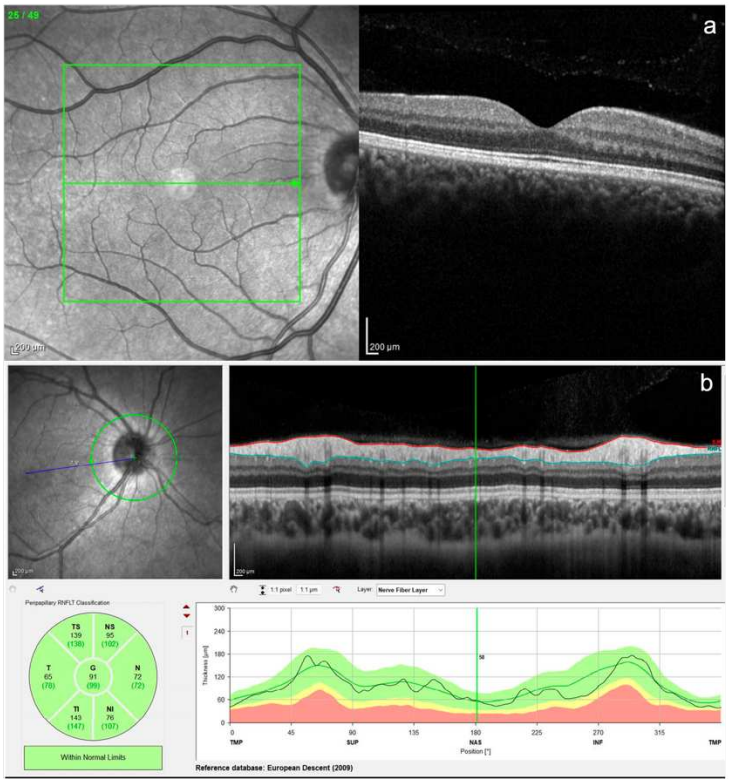

Figure 4: Optical coherence tomography images of two healthy right eyes, in the macula (a) and in the peripapillary area (b), obtained using the Spectralis HRA + OCT2 platform (Heidelberg Engineering, Heidelberg, Germany).

Optical coherence tomography angiography (OCT angiography) is a recent noninvasive imaging technology which uses high speed repeated scans of the same region to detect blood cells' movement and, therefore, vessels, with no need for intravenous contrast injection. Furthermore, OCT

angiography provides tridimensional images of the vascularization and allows for automatic quantitative measurements that can be objectively compared.[7] (Figure 5)

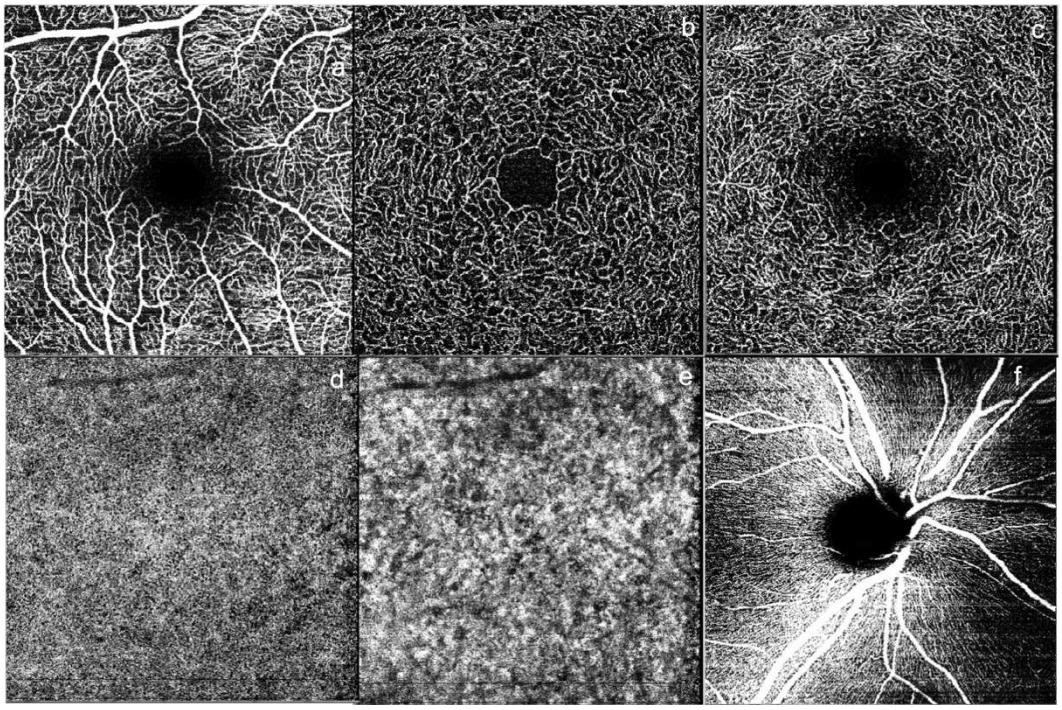

Figure 5: *en-face* optical coherence tomography angiography images of the different retinal plexi obtained using the Spectralis HRA + OCT2 platform (Heidelberg Engineering, Heidelberg, Germany): (a) superficial vascular plexus (SVP), (b) the intermediate capillary plexus (ICP), (c) the deep capillary plexus (DCP), (d) the choriocapillary, (e) the choroid in the maxcular area and (f) the radial peripapillary capillary plexus (RPCP) in the peripapillary area.

With regard to the anterior segment of the eye, corneal confocal microscopy (CCM) is an in vivo technique that allows, in a noninvasive way, the study of all corneal layers, including the sub-basal nerve plexus, which represents part of the peripheral nervous system. Moreover, it may provide a non-invasive quantification of corneal cellular elements, such as the endothelial cells, and of different nerves parameters.[2]

2.2 AMYLOIDOSIS

Amyloidosis includes a group of rare and heterogeneous diseases characterized by the extracellular deposition of amyloid, derived from

different proteins that are destabilized, modified and deposited in different tissues and organs.[8] Abnormal proteins folding lead to a conformational shift into a β-pleated sheet structure consequent to which the protein becomes hydrophobic, insoluble, non-functional, and resistant to degradation. This process derives from the combination of several factors, including a sustained increase in the concentration of proteins with an acquired or hereditary mutation, or wild-type (wt) proteins with an intrinsic propensity to misfold, or a proteolytic remodeling of a wt protein into an amyloidogenic fragment.[9] Deposition of amyloid can occur in the presence of an abnormal protein [e.g. hereditary amyloidosis and acquired systemic immunoglobulin light chain (AL) amyloidosis], in association with prolonged excess of a normal protein [e.g. reactive systemic (AA) amyloidosis and β2-microglobulin (β2M) dialysis-related amyloidosis], and accompanying the ageing process [e.g. wild-type transthyretin amyloidosis (wtATTR or senile systemic amyloidosis)]. More than 30 proteins have been identified to form amyloid in humans, but recent use of mass spectrometry to identify amyloid suggests that many more proteins might be amyloidogenic.[8] The great variety in deposits and subsequent clinical manifestations has brought to the necessity of a consensus meeting to clarify the Nomenclature.[10] Amyloid was defined as *in vivo* deposited material, which can be distinguished from non-amyloid deposits, because of a similar structure, consisting of anti-parallel β-strands (less commonly, parallel β-strands) of fibrils at electron microscopy and typical X-ray diffraction pattern. Amyloid deposits also contain other minor non fibrillary components, including glycosaminoglycans (GAGs), apolipoprotein E and serum amyloid P-component (SAP). This specific structure accounts for their particular affinity in binding Congo red dye, producing a characteristic green birefringence when viewed under cross-polarized light, which remains the histological gold standard for confirming the presence of amyloid in tissue samples.[8,10] Even if amyloid is usually defined as extracellular material, the detection of some intracellular deposits, brought to the extension of the definition also to intracellular fibrils, if they respond to the above mentioned

characteristics.[10] Moreover, it was defined that systemic amyloidosis is derived from a plasma protein, and localized amyloidosis from proteins produced at the site of deposition.[10] With regard the nomenclature of the specific amyloidosis types, it depends on the main protein constituting the fibril and is always designated as “A” plus a suffix, corresponding to the abbreviation of the name of the precursor protein (e.g. AL where L stands for immunoglobulin light chains).[11]

Affected organ biopsy is the most common diagnostic approach, even if it remains an invasive approach with, for example, risk of bleeding. Microscopic amyloid deposits are very widespread in systemic forms of the disease, and abdominal fat aspiration is a simple and innocuous high-yield alternative to target organ biopsy. The sensitivity of fat in amyloid detection is amyloid-type dependent, ranging from 70–90% in AL and 67% in ATTRv to only 14% in ATTRwt amyloidosis.[9] A negative fat aspirate does not exclude amyloidosis, particularly in localized forms, and biopsy of, for example, rectal wall or labial salivary glands are alternatives with reasonable diagnostic sensitivity. Bone marrow biopsy is routinely performed for the diagnosis/follow-up of patients with most hematologic disorders. Confirmation of the type of amyloid fibril is crucial, since this will guide therapy and avoid misdiagnosis among different amyloidosis types.[8,9,12] For typing of amyloid proteins, immunohistochemistry diagnostic value is very high in most cases of ATTR amyloidosis, more than for AL amyloidosis. Immunofluorescence has also been traditionally used and more recently, mass spectrometry. Gene sequencing must be performed when there is any suspicion of hereditary amyloidosis. Assessment or identification of the underlying disorder is the next step in patients with systemic amyloidosis.[8,9]

AL amyloidosis is the most common form of systemic amyloidosis and is due to the deposition of immunoglobulin light chain fragments in tissues. Transthyretin (TTR) -related gene mutation amyloidosis is the most common form of hereditary amyloidosis worldwide.[8,13] AA amyloidosis, is typically associated with an underlying chronic inflammatory process and is

an important cause of systemic amyloidosis in developing countries, due to the high prevalence of associated, underlying, infectious diseases.[9] Few epidemiological data have been published for amyloidosis, and not always concordant.[8,9] The first population-based study of AL amyloidosis was done in Olmsted County, MN, USA, and was published in 1992. It reported the incidence of AL amyloidosis as three to five cases per million population.[8] Prevalence data on amyloidosis have changed substantially over the past two decades. The prevalence of AL amyloidosis in the US has significantly increased between 2007 and 2015, reaching an estimate of about 40.5 per million.[9] Conversely, a progressive decrease has been suggested in the proportion of patients referred with AA amyloidosis due to improvement of treatment of inflammatory diseases (e.g. arthropathies). Referral of patients with ATTRwt amyloidosis has significantly increased, which probably reflects the increasing consciousness of the disease among physician and the contribution of advanced diagnostic modalities such as cardiac magnetic resonance imaging (MRI). The true incidence of ATTRwt amyloidosis in elderly people remains unknown, but cardiac amyloid deposits of this type have been reported at autopsy in a quarter of individuals older than 80 years. The global prevalence of ATTRv is estimated as 5000 to 50000 but higher number have been also reported and it varies among populations, according to the frequency of different mutations but probably also other, still unknown, genetic and environmental factors.[9,14,15] In fact the prevalence and the penetrance of the same mutation may significantly vary among different populations, even when endemic.[8]

The potential for amyloid deposits to affect almost any organ system accounts for the high variability in clinical features of systemic amyloidosis, which are rarely specific to one type of amyloidosis, leading to difficulties and delays in diagnosis. Advanced organ dysfunction is often detected by the time of the clinical diagnosis, so keeping a high index of suspicion is important for early diagnosis. Specific combinations of symptoms should trigger suspicion for a diagnosis of amyloidosis.[8] Therefore, the better

definition of the possible clinical manifestations of the different forms of amyloidosis is of primary relevance, including the ocular features.

There is a high number of amyloidosis types with significant clinical manifestations [fibrinogen A α chain, hereditary AApoA1, lysozyme (ALys) amyloidosis, AA amyloidosis etc] but the main focus of this study will be ATTR amyloidosis and the comparison with the most frequent systemic form, AL.[8]

2.3 AL AMYLOIDOSIS

Light-chain amyloidosis is a rare disease (2200 new cases every year in the US) caused by a clonal plasma cell disorder associated with multiorgan deposition of fibrils which are derived from monoclonal immunoglobulin light chains.[8,12] AL amyloidosis is most frequently caused by plasma cell dyscrasia or can occur in association with light-chain producing lymphoproliferative disorders, e.g. multiple myeloma.[8,9,16] It may also, more rarely, occur as a localized lesion without any other systemic manifestation. Common sites of localized lesion include the respiratory tract, bladder, eyelids, and skin. In these cases, the amyloidogenic immunoglobulin light chain is produced by a clone of plasma cells present at the site of amyloid deposition and no precursor protein is found circulating.[8]

Systemic clinical manifestations include renal involvement, cardiomyopathy with heart failure and arrhythmias, hepatomegaly, neuropathy, and bleeding diathesis, however virtually all organs may be involved.[8,16,17] Cardiac involvement occurs in about 50-70% of patients with AL amyloidosis and it is the leading cause of morbidity and mortality, typically presenting as restrictive cardiomyopathy, often with important signs of right ventricular failure (oedema, raised jugular venous pressure, and congestive hepatomegaly). Patients with AL amyloidosis are often more symptomatic than patients with other types of amyloidosis, which supports in-vitro

evidence of significant myocardial cell toxicity of amyloidogenic light chains in this subtype.[8,9]

The renal involvement is one of most common complications of AL amyloidosis (as well as in other forms, e.g. AA, fibrinogen A α-chain, ALect2, and AApoA1 amyloidosis). Albuminuria, which often progresses to nephrotic syndrome, is typical, but renal dysfunction may remain asymptomatic until it is very advanced.[8] Amyloid peripheral neuropathy with predominantly axonal involvement has also been described, involving both the small and large fibers. It begins with loss of the small fiber-mediated sensations of heat or cold, pain, and may be difficult to differentiate from other inflammatory polyneuropathies. Autonomic neuropathy symptoms are also reported, such as postural hypotension, early satiety, and diarrhea or constipation. About a fifth of all patients with systemic AL amyloidosis have peripheral neuropathy at presentation.[8] Involvement of soft tissues, apart from carpal tunnel syndrome, is peculiar of AL amyloidosis, including macroglossia, muscular pseudohypertrophy, enlargement of the salivary glands, and submandibular soft-tissue infiltration. Serum cardiac biomarkers are an important validated method for risk stratification and staging in AL amyloidosis.[8]

Treatment of AL amyloidosis is directed against the underlying diseases which can range from benign monoclonal gammopathy of undetermined significance (MGUS) (which does not otherwise need treatment), to frankly malignant plasma cell proliferation (e.g. multiple myeloma). Therefore, treatment includes combination chemotherapy regimens that targets the underlying clonal plasma cell disorder, with the aim of rapidly reducing production of amyloidogenic light chains to limit progressive damage to amyloidotic organs.[8,16] The reduced functional reserve of amyloidotic organs and poor performance status results in much greater treatment toxicity in AL amyloidosis, so a risk-adapted approach to treatment is critical. Median survival in patients with AL amyloidosis has nearly doubled over the past decade, even if it remains a devastating disease. New therapeutic

strategies are under study, such as therapeutic antibodies to target amyloid deposits directly.[8,18]

Ocular signs have been described, more frequently after the diagnosis of systemic manifestations but also as presenting features, with a prevalence between 10% and 20%. However, it remains difficult to have clear data on the prevalence and natural history of these alterations in the context of the disease because of the limited percentage of patients undergoing regular ocular examinations and the variability of the described populations.[17] In AL amyloidosis, amyloid deposition can involve several ocular sites, including the eyelid, conjunctiva, lachrymal gland, ocular adnexa, orbit, and extraocular muscles. Temporal artery involvement has also been described. A typical, although rare, sign of ocular involvement is the appearance of bilateral periorbital purpura or ecchymosis, usually appearing late in the course of the disease.[17,18]

Upper and/or lower eyelid swelling with tearing, discomfort, and foreign-body sensation, proptosis, thickening and hyperemia of the bulbar conjunctiva, salmon-like plaques in the tarsal and/or bulbar conjunctiva, recurrent subconjunctival hemorrhages, lachrymal gland enlargement, ptosis and ocular displacement due to the presence of an orbital mass are the most frequently reported symptoms. In the more severe cases, the involvement of one or more of the extraocular muscles results in motility deficits, diplopia or ophthalmoplegia.[19] When the temporal artery is involved either uni- or bilaterally, typical signs such as jaw claudication, headache, blurry vision, and diplopia may be present. Amyloid infiltration into the trabecular meshwork may result in glaucoma. The correct diagnosis is established based on an incisional punch or wedge biopsy followed by an immunohistochemical analysis of the specimen. Asymptomatic patients can be kept under observation, whereas most patients with signs and symptoms undergo surgical debulking of the mass, or, more rarely, radiotherapy.[17]

2.4 TRANSTHYRETIN AMYLOIDOSIS

Transthyretin amyloidosis is a progressive systemic disorder caused by misfolding of the TTR protein leading to protein aggregation and the formation of amyloid fibrils and, ultimately, to deposition in affected organs, most commonly the heart and the peripheral nerves. It can arise from mutated TTR or wild-type TTR protein deposition.[13,20] Transthyretin is a homotetrameric protein of 55 kilodalton (kDa) which is mainly found, as a stable tetramer, in plasma, cerebrospinal fluid and aqueous humor and thought to be synthesized mainly in the liver (90%), but also in choroid plexus, RPE, and pancreas. The TTR gene is located on chromosome 18 (18q12.1).[4,21,22] Previously known as “thyroxine binding prealbumin”, in 1981, its name was changed to ‘‘transthyretin’’ by the International Union of Biochemists since the physiologic role of the protein as thyroxine and retinol transporter was established.[4]

In vitro studies have demonstrated that TTR forms amyloid fibrils through a process that involves tetramer dissociation followed by misfolding of the released monomers into an aggregation-prone conformation by which oligomers, soluble aggregates, insoluble amorphous aggregates, leading to amyloid fibrils formation. Tissue culture studies have shown that TTR monomers or small oligomers (nonfibrillar TTR) are the real cytotoxic elements to the cells, compared to the native tetramer, large soluble aggregates, and amyloid fibrils.[4,23] Recent studies have reported that TTR has a protective role in transgenic murine models of Alzheimer’s disease. It has been suggested that it may reduce the toxicity of the antibodies oligomers or decrease their formation, perhaps having a generic chaperone-like function within neurons as well as in the extracellular space of the brain. Several studies, although not all those reported, have found decreased TTR levels in the cerebrospinal fluid of patients with Alzheimer’s disease.[4] Moreover, some reports suggest that TTR may play a role in the pathogenesis of type 1 and type 2 diabetes, even if with contrasting results.[4] These data suggest more complex mechanisms at the base of TTR amyloid toxicity. In fact, in the course of studies directed at finding small molecules that could stabilize the native tetrameric TTR conformation to

prevent amyloid formation, it has become apparent that TTR has the capacity to bind a variety of structures in its thyroxine (T4) binding pocket. It is possible that evolution has maintained such versatility in order to allow TTR to perform a multiplicity of biologic functions.[4]

The clinical syndromes associated with TTR aggregation are the hereditary form of ATTR, in which point mutations in the gene encoding the protein result in deposition of aggregates in many tissues, such as peripheral and autonomic nerves and heart, and “senile” systemic amyloidosis (ATTRwt), a late onset disease in which the wild-type protein deposits primarily in the heart, but also in other organ, including the gut and carpal tunnel.[4,24] The clinical manifestations of ATTRv usually have an earlier onset than ATTRwt presumably due to the decreased stability of variant TTR with respect to the wt protein, with the most aggressive variants depositing as early as the second decade of life.[4] Moreover, the two different syndromes may significantly differ in clinical manifestations. Neuropathy and cardiomyopathy are common manifestation of ATTR amyloidosis and are associated with a particularly poor life expectancy of 2 to 6 years after diagnosis.[15] Cardiac involvement is, for example, a dominant feature in patients with ATTRwt but it is rare in patients with Val30Met mutation-associated disease.[8] Moreover, different phenotypes have been described also in ATTRv, suggesting that there are several contributing factors to the phenotype, either environmental or genetic.[13]

The diagnosis of ATTR is still a significant challenge for physicians. Because of the variety of clinical manifestations and the not widespread awareness of the disease among different centers, common misdiagnoses may include idiopathic axonal polyneuropathy, chronic inflammatory demyelinating polyradiculoneuropathy, lumbar spinal stenosis, as well as diabetic or chronic alcoholism induced polyneuropathies.[25] It may be the case that patients presenting with inconsistent autonomic symptoms are later identified as new clinical phenotypes.[26] Moreover, the incorrect differentiation among amyloidosis deposits, may lead to misdiagnosis with more frequent amyloidosis types, leading to incorrect management.[12] For

example, a significant proportion of ATTR patients also have MGUS, which may lead to a misdiagnosis of AL amyloidosis.[9] A diagnosis delay of years is frequently reported in ATTR, although onset before 45 years and positive family history are factors associated with earlier diagnosis.[27] Particularly for sporadic or scattered cases, a lack of awareness among physicians of possible clinical features and limited access to diagnostic tools (i.e., pathological studies and genetic screening) can contribute to even higher rates of delay and misdiagnosis. However, the timely initiation of appropriate treatment is particularly important, given the rapidity and irreversibility with which ATTR can progress if left unchecked, as well as the limited effectiveness of available treatments during the later stages of the disease.[20]

Following a clinical suspicion, positive results from both biopsy and genetic analysis are essential to distinguish ATTR from the large number of peripheral neuropathies and cardiomyopathies, formally diagnose it, and eventually specify the genetic variant.[19] Moreover, patients usually require extensive and multidisciplinary examinations to correctly manage ATTR complications.[25,26]

2.4.1 Hereditary transthyretin amyloidosis

ATTRv amyloidosis was first described as familial amyloid polyneuropathy associated with TTR (TTR-FAP), in Portugal in 1939 on a population of 74 patients from Pòvoa de Varzim. Later, other cases were identified in Japan and Sweden, which remain endemic areas, even if the disease has been now recognized worldwide. Another significant clinical manifestation associated with TTR mutations which has been frequently described is cardiomyopathy, with an estimated prevalence of about 40000 of the 50000 ATTRv persons globally.[15] However, these two clinical syndromes belong to the broader disease spectrum of ATTRv amyloidosis and the distinction is less commonly used, and the concept of “mixed phenotype” has been introduced because varying severity grades of different clinical manifestations (including cardiomyopathy, carpal tunnel syndrome,

autonomic neuropathy, vitreous opacities, kidney disease, meningeal involvement etc) are present and have been recognized in ATTRv amyloidosis, thanks to the greater medical consciousness of the disease and the diagnostic approaches.[20,26] Some of these manifestations may even be the first clinical signs in some ATTR variants.[26] The majority of patients are male heterozygous carriers.[9]

Currently more than 150 mutations have been associated with ATTRv amyloidosis, and even though transmission is autosomal dominant, the penetrance is variable and increases with age.[22,28,29] Approximately 70% of patients worldwide carry the Val30Met mutation, endemic in Japan, Portugal, Sweden, making it the commonest and the most studied mutation worldwide. Two different populations have been related to this mutation, defined by the reported age at onset, either before or after the age of 50 years: the early-onset (typical in Portugal) and the late-onset (typical in Sweden) phenotypes, which may be influence by still unknown genetic and environmental factors in the clinical expression and the age of onset. Val30Met ATTRv amyloidosis seems to be associated, particularly in the early-onset form to somatic and autonomic peripheral nerve dysfunction followed by cardiac conduction defects, while the late-onset one to more significant cardiomyopathy, large and small-fiber sensory neuropathy with only mild autonomic dysfunction. The Val30Met variant seems to be also the most common mutation in northern and central Italy.[13,14,22] The mean survival time, without therapy, in the early-onset and late-onset Val30Met patients is about 12 years and 7 years respectively.[23] The most common north american mutation Val122Ile tends to present as pure or predominant cardiomyopathy in late middle age. Other mutations have been described, associated with milder phenotypes, such as Arg104His and Thr119Met, as well as mutations associated with more aggressive phenotypes, such as Leu55Pro.[13,22] About half of all cases of ATTRv amyloidosis do not have a family history and are designated as sporadic cases.

Families originating from endemic areas of Portugal and Japan, where the prevalence of 1/500 to 1/10000 have been reported, usually have earlier diseases onset of the disease with higher penetrance.[22,29] The lag time between the onset of symptoms and ATTRv amyloidosis diagnosis may vary from 2 to 6 years.[24] ATTRv requires a biopsy and pathological exam to demonstrate amyloid deposits. Nerves, heart, kidney, colorectal mucosa, abdominal fat aspirate, or salivary glands can be biopsied.[21] Tissues are stained with hematoxylin and eosin to reveal homogeneous eosinophil extracellular areas and with Congo red to confirm green birefringence, when viewed under polarised light. Immunohistochemistry can also be used to confirm the ATTR composition of amyloid. For a reliable formal diagnosis and to specify the genetic variant, genetic testing is necessary.[20,22,27] Moreover, in some cases of localized ATTRv amyloidosis, diagnosis may be provided only by genetics, with a negative biopsy.[26,27]

The clinical manifestations of ATTRv amyloidosis are highly variable. The average age for onset of symptoms is around 33 but it can vary from age 17 to 78. Initial symptoms are typically autonomic sensorimotor neuropathy, including paresthesia, decreased thermal and pain sensitivity in the extremities and in the cornea, afferent ataxia, and autonomic dysfunction. Neuropathy is usually symmetrical with focal distribution and centripetal progression. At the late stage, suffering flaccid paralysis of the limbs, multiorgan dysfunction, and autonomic dysregulation occur.[22,30] The stages of ATTRv amyloidosis severity are graded according to patients' walking disability and degree of assistance required. The features of neuropathy change based on the type of ATTRv amyloidosis (early or late onset) and stage of disease.[30]

Cardiac involvement includes serious conduction disorders with the risk of sudden death and infiltrative cardiomyopathy. Electrocardiograms (ECG), Holter-ECG, and intracardiac electrophysiology study are helpful to detect conduction disorders. Echocardiograms, cardiac magnetic resonance imaging, scintigraphy with bone tracers, and biomarkers (e.g., brain

natriuretic peptide, troponin) can all help to diagnose infiltrative cardiomyopathy.[20]

Digestive and ocular involvement often follow the cardiac and neurological manifestations with renal signs appearing later in the natural course of this disease. The importance of routine ophthalmological examinations has already been underlined in ATTRv amyloidosis patients, as many patients may show no signs of involvement at first, but may develop a wide variety of alterations as the disease evolves, many of them being treatable if detected in time.[28]

Presymptomatic genetic testing may be of value in increasing survival, since patients will be able to access treatment in useful time, before the disease progresses.[22,26]

2.4.2 Wild type transthyretin amyloidosis

ATTRwt amyloidosis is characterized by the deposition of TTR in tissues and organs in its native conformation. In fact, due to the amyloidogenic nature of the monomeric form of the TTR protein, ATTR amyloidosis can also occur despite lack of any mutation, possibly because of an age-related reduced effectiveness of the protein folding quality control systems.[9,31] This subtype is characterized mainly by clinical manifestations in elderly men (more than women) with higher prevalence in more advanced age, reason why it has long been referred to as “senile” amyloidosis. The cardiac involvement has long been considered the major and almost exclusive manifestation of this form. In particular the typical presentation is with hypertrophic heart failure, with relatively preserved systolic function early in the disease.[13,32] However, carpal tunnel syndrome and spinal stenosis have also been observed in ATTRwt amyloidosis, several years before the onset of systemic symptoms.[31,33] The deposition of ATTRwt amyloid is found in about one third of elderly people undergoing carpal tunnel decompression and the high prevalence of tunnel carpal syndrome in ATTRwt patients has been confirmed in different studies.[31,34] Therefore, at present a history of carpal tunnel syndrome anticipating unexplained

symptoms of heart failure in elderly patients should raise suspicion of ATTR amyloidosis.[8] The association with peripheral neuropathy and skeletal myopathy have also been recognized.[13]

A significant prevalence of abnormal findings at neurological evaluation, according to the Neuropathy Impairment Score (NIS), has been confirmed, even after excluding patients with comorbidities. The results may have been influenced by the high mean age of ATTRwt patients, with high prevalence of carpal tunnel syndrome and concomitant conditions related to aging (i.e., rheumatologic disorders involving the spine and limb extremities) that may potentially be responsible for reduced hand mobility or sensory impairment.[33] However, in some ATTRwt patients also an increased nerve cross-sectional area at ultrasound has been proved, which has been suggested as a longitudinal biomarker of both disease progression in ATTRv amyloidosis and disease occurrence in pre-symptomatic carriers.[33,35] Electrodiagnostic evidence of peripheral neuropathy in patients with no other causes of neuropathy also confirmed that peripheral large nerve fiber involvement may occur in ATTRwt amyloidosis. Moreover, reduced sudomotor function was observed and small fiber involvement, particularly autonomic dysfunction, was suggested to significantly influence the systemic manifestations (i.e., fatigue of heart/kidney failure), eventually playing a role in the severity and course of the disease.[33] The comparison between ATTRwt patients and age-matched controls found a higher prevalence of carpal tunnel syndrome, spinal stenosis and polyneuropathy in the first ones with evidences of sensory, sensorimotor and asymptomatic neuropathy at electrophysiology, suggesting the necessity of a through neurologic evaluation in patients with cardiac ATTRwt amyloidosis.[34]

Compared to ATTRv amyloidosis, heart failure has been reported to be usually less severe and disease progression slower, despite morphological similarities by echocardiography and magnetic resonance imaging. This has been linked to the possible inferior toxicity of ATTRwt compared to the mutant-type ATTR, resulting in earlier and more severe organ manifestation.[31] In fact, it was reported that, in patients with Val30Met

mutation, the circulating monomers are mostly wild-type, thus not resulting from the mutation and identical to those produced in senile systemic amyloidosis. This may be due to the fact that the mutant molecules are more unstable than the wt ones and therefore more prone to aggregation. However, the fact that circulating monomers are mostly wild-type could also simply result from the faster elimination of the mutant molecules. Anyway, this suggest that the conformation and behavior of ATTR fibrils differ in ATTRwt and ATTRv amyloidosis.[22]

2.4.3 Transthyretin amyloidosis and the eye

Pathophysiology of ophthalmologic involvement in ATTRv amyloidosis was originally presumed to be the same as for cardiac and neurological disease and that it was due to a local deposition of abnormal TTR from the liver. However, with the first clinical evidences obtained after the introduction of liver transplantation as a treatment for ATTRv amyloidosis, it became clear that the ophthalmological involvement in patients undergoing transplantation not only did not improve but worsened. Therefore, it is now evident that a majority of ATTR causing the ocular manifestations in ATTRv amyloidosis derives from the eye itself.[28,36]

In the eye, TTR is highly transcribed and translated in the RPE, which is the site of reformation of 11-cis-retinal from all-trans retinol, after phototransduction. The source of all-trans-retinol in RPE is ultimately the liver which secretes retinol bound to the TTR–retinol binding protein (RBP) complex. In RPE, free retinol uptake seems to be mediated by a retinol-RBP cell membrane receptor which is highly expressed in the basolateral side of these cells. TTR is synthesized and secreted from the apical side of the cell layer (i.e. the interphotoreceptor matrix, IPM). It has been speculated that TTR–RBP in the IPM might serve as transporters of retinol to other cells, like retinal amacrine and Müller cells, which contain cellular retinoic acid binding protein and presumably require all-trans-retinol as a precursor. In vitro, the TTR:RBP secretion ratio of RPE to the IPM is 50:1. If the same

ratio exists *in vivo* it implies that there is an excess of TTR in the IPM. Moreover it has also been suggested that TTR might also function as a carrier of T4 during the development of the eye.[4]

Chromatographic analyses on rats eyes showed that choriocapillaris significantly restricts plasma TTR from crossing Bruch's membrane into the retina.[37] Therefore, it confirms that retinal ATTR is mainly derived from the RPE.[21] However, the possibility of slow accumulation of plasma ATTR within the retina may not be excluded, and it could also involve the more anterior portions of the eye.[21] Some studies have also suggested that amyloid deposits in the anterior segment of the eye are produced by the pigmented ciliary epithelium, while vitreous deposition originates from the RPE.[16] It is also known that the metabolic exchange and equilibration between the systemic circulation and the vitreous humor is very slow, confirming that the source of variant ATTR deposition in the vitreous is probably the RPE.[4,22]

Studies on rats showed that TTR mRNA is localized exclusively in the RPE. However, immunohistochemistry demonstrated that ATTR has a more widespread distribution in the rat eye, including the ciliary epithelium, iris epithelium, corneal endothelium, optic nerve fiber layer of the retina, vitreous humor, lens capsule and lacrimal gland and also in other ocular structures, with varying intensity of immunoreactivity.[21] Moreover, the differential immunoreactivity of ATTR in different cells structures (e.g. ganglion cells vs cornea or RPE) suggested that ATTR may have a different behavour, according to association of ATTR with different macromolecules in various cell types. In fact, multiple fibril morphologies have been demonstrated in the eye even within the same type of pathology. The reason for variation in fibril protein structure could be either patient-specific, or due to modifications induced by the local microenvironment of the specific organ. This may explain the various patterns of ocular amyloidosis which have been described in ATTR amyloidosis.[21,38]

Histopathological studies confirmed the presence of amyloid deposition in autopsied ATTRv eyes with different amyloid distribution patterns but some

consistencies of the deposition. The most frequently involved tissue was the conjunctiva, in the early stage of the disease, with deposits macroscopically correspondent to abnormal conjunctival vessels. Amyloid deposits in the iris were found in about one third of patients. The deposits were found also in the retina/vitreous in less than 10% of ATTRv patients in late stages, while in the optic nerve in the early stages. The degree of amyloid deposits did not seem to be correlated with the duration of the disease or age.[39]

Several ocular manifestations have been described in ATTR amyloidosis, although mainly in case-series and single case reports and mainly in ATTRv amyloidosis. Furthermore, a still underdiagnosed aspect of amyloidosis is the involvement of small fibers which can significantly change the quality of life of patients and which requires early diagnosis for correct patient management.[13,34] Moreover, ATTRwt amyloidosis has been less studied to date, particularly from an ophthalmological point of view.[13]

In particular, ocular manifestations have been reported in 10-40% of patients with ATTRv amyloidosis, usually occurring later during the course of the disease, with no clear correlation with neither the systemic symptoms nor the duration of the disease or treatment.[22,28,36] However, also cases of amyloid deposit in the vitreous without systemic manifestations have been described.[22,39] As reported above, because of the possible different associations of ATTR with different cells' structures, various patterns of ocular amyloidosis have been described.[21] The main ocular manifestations reported in ATTRv amyloidosis patients include vitreous opacities, open-angle glaucoma, abnormal conjunctival vessels, keratoconjunctivitis sicca and loss of corneal sensitivity and neurotrophic corneal ulcer, anterior capsule opacity of the lens, retinal vascular changes, pupillary light-near dissociation, irregular pupil, optic neuropathy.[22,40] However, a variety of other manifestations have been suggested to be linked to the disease, such as retinal and choroidal neovascularization.[41]

The amyloid deposits in the vitreous have been largely reported in ATTRv amyloidosis, occurring either during the natural course of the disease or after hepatic transplantation, with a variable prevalence and time of

occurrence in patients with different mutations [e.g. Tir114Cis and Lys54 mutations vs Val30Met (rarer)].[4,22,28] It is possible that the GAG hyaluronic acid in the vitreous promotes mutant ATTR deposition as occurs for other amyloidogenic proteins, e.g., gelsolin.[4] In some cases they may cause gradual decrease in visual acuity even requiring a surgical approach through vitrectomy, even if vitreous opacities may recur even after the intervention.[22,28] However, vitrectomy may also increase oxidative stress in the trabecular meshwork and, in the absence of vitreous, the amyloid aggregates may reach the trabecular meshwork and Schlemm's channel more easily and deposited in both structures, leading to intraocular hypertension. Thus, studies suggest that the vitreous acts like a filter which retains the amyloid fibrils and prevents their progression to the trabecular meshwork. This underlines the complexity of the ocular picture in ATTR patients, requiring a careful therapeutic approach considering all the pathologic components. For example in these patients an incomplete vitrectomy for clinically significant vitreous opacities has be suggested, to delay the progression of glaucoma, but not all Authors agree.[22,42]

One of the main causes of irreversible blindness in amyloidosis patients is open angle glaucoma. The pathophysiological mechanisms responsible for the elevation of intraocular pressure (IOP) include perivascular amyloid deposition in conjunctival and episcleral tissues, intra-trabecular deposition, and deposition of amyloid on the pupillary edge, which may precede glaucoma by months or years.[22] Moreover, in ATTRv amyloidosis the curse of the disease seems to be more aggressive, with a possible explication in the reduction of physiological neuroprotective substances, such as erythropoietin, compared to open angle glaucoma patients without ATTRv amyloidosis.[22,43] Also the continuous production of ATTR can explain the difficulty in control IOP, with higher percentage of patients requiring a surgical approach than patients without ATTR amyloidosis.[22]

Abnormal conjunctival vessels, described as red dots and segmental and fusiform dilatation of conjunctival vessels, are reported in a high percentage of patients during the disease. These changes seem to result from liver

synthesis of ATTR, not from intraocular production, and there is no progression after liver transplant.[22]

Dry eye may be the result of either autonomic neuropathy or amyloid deposition in the lacrimal gland, contributing to neurotrophic keratopathy and cornea perforation, which has been described in some cases. In fact, progressive loss of corneal sensitivity and subsequent damage to the epithelium and stroma occur during the disease.[22,44] A damage of small nerve fibers of the cornea has been recently described using CCM in ATTRv amyloidosis patients, even if often only with a qualitative evaluation of the nerve alterations.[45] Rousseau et al. were able to analyze some CCM quantitative parameters and found the corneal nerve length to be reduced in ATTRv amyloidosis compared to controls.[46] Moreover they found that corneal nerve fiber length correlated with the severity of both sensorimotor and autonomic neuropathies in ATTRv amyloidosis, as well as with clinical motor neuropathy and walking status and with IntraEpidermal Nerve Fiber Density in the lower limbs.[46]

Intraocular production of ATTR leads to amyloid deposition in the anterior lens capsule, that is often asymmetrical between the two eyes, and at the pupillary edge, leading to a peculiar aspect of pupil, known as pupillary scalloping.[21,22] These conditions may impair spatial contrast sensitivity and may lead to early presbyopia, requiring higher diopter addition and are not influenced by liver transplantation.[22] This may be related on the one hand to a loss of lens elasticity and on the other to autonomic neuropathy, which affects the ciliary muscle accommodation. Moreover, pupillary light-near dissociation has also been described, explained by the deposition of amyloid in the iris.[22]

Retinal changes have been less frequently described in ATTRv patients, particularly linked to some mutations.[47] Hemorrhages or cotton wool spots have been detected, as well as retinal and choroidal amyloid angiopathy, characterized by vessels abnormalities, hyperfluorescent foci along the vessels at the angiography, vascular occlusions.[48–50] Also, alterations of the outer retina and the vitreoretinal interface have been detected at OCT

in ATTRv patients as well as significant abnormalities of scotopic and photopic electroretinography. These were supposed to be related to the impairment in the visual cycle because of a malfunction of ATTR protein.[45]
Medrano JR et al reported the presence of clinically detected (and not histologically proven) amyloid deposits in a population of 18 ATTRv patients, in crystalline lens (22.2%), retinal vessels (22.2%) and in retinal parenchyma (55.6%), with atrophy secondary to vascular occlusion in inner retinal layers in all patients with vessel deposits and vitreous-retinal tractions causing an advancing retinal schisis in one eye.[28]
ATTR is a minor component of drusen, extracellular deposits of material found in the Bruch's membrane, which lays between the RPE and the choroid of the eye, and are increased in age-related macular degeneration (AMD). It is possible that in this case the source of ATTR is the systemic circulation rather than the RPE. Circulating RBP charged ATTR may be predisposed to dissociation at the time of delivery of retinol to the RPE with the subsequent generation of monomeric ATTR, the aggregate precursor. Alternatively, it has been suggested that TTR may be trapped in the drusen when its concentration is lower than that required to prevent drusen formation or enhance their clearance.[4]
A rare cause of blindness in these patients is optic neuropathy, which has also been described in a bilateral form, after excluding other diagnostic hypotheses, such as vitreous opacity or glaucoma. It is probably caused by ischemia secondary to amyloid deposition in small vessels, as well as impairment of autonomic self-regulation.[22,44,51]
All the ocular manifestations are reported mainly in case series and case reports of ATTRv patients, often with different mutations prevalence and possible systemic confounding factors (e.g. diabetes). Therefore, the prevalence, time of onset and evolution of these features still need to better delineate. Moreover, they have been only anecdotally reported in ATTRwt amyloidosis.

Ocular signs and symptoms may be the most prevalent but also the only manifestation of rare forms of amyloidosis such as gelsolin-, keratoepithelin- and lactoferrin-related amyloidosis.[17]

2.4.4 Transthyretin amyloidosis treatment

The management of ATTR amyloidosis has significantly changed in recent years, with the advent of new pharmacotherapeutic alternatives besides liver transplantation (for ATTRv amyloidosis).[20] Therapeutic options in a patient with ATTR amyloidosis depend on the stage of the disease and the patient's age. In patients with a positive family history, presymptomatic medical assistance is of utmost importance, since the available treatments are more effective in the early stage of the disease.[22] Targeted therapy is essential in the first instance to prevent further production of amyloid deposits. Thereafter, symptomatic therapy of sensorimotor and autonomic polyneuropathy and cardiac, renal, and ocular injury is required. Finally, genetic counselling to patients and relatives is recommended.[20]
The first liver transplant for ATTRv amyloidosis was performed in 1990 on a male Swedish patient. Liver transplantation removes the main source of ATTR, resulting in the fast decline of ATTR concentration to levels around 1%. Thus, it has proved to halt the progression of neurological symptoms and prolong patient survival, as long as it is performed at an early stage. The introduction of liver transplantation has doubled the survival rate from 10 to 20 years.[20,22] Although organ transplantation can be a lifesaving procedure in ATTRv patients, careful selection and counselling of patients are important. Procedure-related morbidity can be high due to amyloidotic organ damage; additional risks are associated with long-term immunosuppression, including secondary malignancies and renal impairment. Moreover, liver transplantation replaces the mutant type with ATTRwt, it does not prevent progression of cardiac disease because the ATTRwt may continue to further expand existing amyloid deposits in the heart. Therefore, continued follow-up of the cardiac system is suggested

and eventual associated cardiac transplantation.[8,20] Furthermore, the ATTR mutated form continues to be produced through the choroid plexus and the RPE and the ciliary body in the cerebrospinal fluid and in the eyes, respectively.[22] In fact, greater prevalence of amyloid deposition in the lens, vitreous body, and glaucoma was observed in the transplanted patients. The first manifestation observed was dry eye, followed by deposition of amyloid in the iris and anterior capsule in the lens and abnormal conjunctival vessels. The vitreous deposition and glaucoma appeared later. The last manifestation was retinal amyloid angiopathy.[22,52]

Not all patients are candidates for liver transplantation, particularly for patients over 65 years of age, those in an advanced stage of disease, or those with heart failure. Liver transplantation is an option also in patients with senile systemic amyloidosis due to the continuous deposition of ATTRwt.[8,22]

Several very promising therapies are under development for ATTR amyloidosis. In-vitro studies showed that the amyloidogenic misfolding of TTR can be inhibited by compounds that bind TTR in the plasma to maintain its normal soluble native tetrameric structure. Tafamidis, a stabilizer of the TTR tetrameric form, has been developed specifically to treat ATTR amyloidosis to slow the progression of ATTR amyloidogenesis by stabilizing the mutant TTR tetramer. Clinical trials have demonstrated its efficacy, with adverse effects similar to those in the placebo group.[20,22] In 2011 Tafamidis was approved by the European Medicines Agency (EMA) for the treatment of peripheral nerve impairment in adults with ATTRv amyloidosis, at the dosage of 20 mg of Tafamidis meglumine, and in 2019 for the treatment of transthyretin-mediated cardiomyopathy both in ATTRwt and ATTRv amyloidosis, at the dosage of 61 mg of Tafamidis.[53]

Diflunisal, a non-steroidal anti-inflammatory drug, binds to ATTR and prevents amyloid fibril formation. It acts on the wild variant of ATTR. According to clinical trials, it stabilizes ATTRv amyloidosis patients, reduces the neurological progression, and maintains the quality of life, without

showing any adverse effects at 2 years compared with placebo. Doxycycline and tauro-ursodeoxycholic acid have been proposed to interfere with the process of ATTR fibrillogenesis.[20]

The liver is the anatomical site most efficiently targeted by novel RNA-inhibiting therapies, which reduce pathogenic ATTR protein levels through silencing of the TTR gene. Two such approaches are now in clinical development: small interfering RNA (siRNA) therapy and anti-sense oligonucleotide therapy.[8] In particular, two new drugs have been approved for ATTRv amyloidosis: patisiran is a siRNA molecule and inoserten is an antisense oligonucleotide, resulting in significant improvement of neuropathy and cardiomyopathy compared to placebo-treated controls.[14,54] Recently, vutrisiran, another small interfering RNA, has shown to be non-inferior to patisiran for the treatment of the polyneuropathy in ATTRv amyloidosis adults, at 18 months follow-up, with a lower frequency of injections. Therefore, the therapeutic approach with siRNA confirmed to be effective in improving neuropathy and quality of life in ATTRv patients.[55] Vutrisiran has been recently approved by EMA for the treatment of polyneuropathy caused by ATTRv amyloidosis (2022).[56]

However, out of the currently approved treatments, tafamidis is the only one that crosses the blood-brain barrier, but only in minimal part, limiting the effects on the central nervous system and the eye. Therefore, studies are needed to understand how to target these two central compartments and selectively reduce the expression of the mutant but not the physiologic TTR form.[54] Recently it has been shown in a small number of ATTRV30M patients receiving tafamidis meglumine (20 mg/d) that tafamidis was present in both cerebrospinal fluid and vitreous humor at levels lower that those found in plasma. While it was not clear whether the concentrations were sufficient to inhibit local ATTR fibrillogenesis, it has been suggested that individual variation in ocular penetration of the drug might be responsible for different manifestations among patients.[36,57]

3 AIMS

The primary aim of this study was to analyze the ocular involvement in ATTRwt amyloidosis, also in comparison with the hereditary ATTR and the AL forms of amyloidosis.

The secondary aim was to identify signs of damage at the level of specific structures, such as the corneal nerve fibers and the retinal vascularization, more difficult to analyze at a systemic level, using non-invasive imaging modalities.

4 METHODS

4.1 Population

This was a cross-sectional, non-interventional study. Patients affected by ATTR or AL amyloidosis referred to the Department of Neuroscience of the University of Padua were included. Inclusion criteria were: age ≥18 years and diagnosis of amyloidosis, including ATTR-related, hereditary or wild-type, or AL amyloidosis. Exclusion criteria were: poor collaboration or presence of disabilities that made the procedures difficult to perform or prevented adequate patient's collaboration; allergy to mydriatics.

Patient records were reviewed for describing the systemic involvement of amyloidosis, the eventual presence of genetic mutation and detecting other systemic comorbidities, such as diabetes to be taken into account as potential confounders in planned analysis. An age-matched control group was also studied, including subjects without story of known significant systemic (e.g. uncontrolled hypertension and diabetes) and ocular diseases.

The study was conducted in adhesion to the Tenets of the Declaration of Helsinki.

All patients underwent a complete eye examination, including best-corrected visual acuity assessment (BCVA), anterior segment examination, evaluating in particular the presence of any deposits and alterations involving the iris and the lens, intraocular pressure, fundus examination, optical coherence tomography (OCT) and OCT angiography and *in vivo* corneal confocal microscopy (CCM). All examinations were carried out in both eyes if they met the inclusion criteria.

4.2 Visual acuity

Best corrected visual acuity (BCVA) was assessed for each eye separately, according to the Early Treatment Diabetic Research Study (ETDRS) protocol, using appropriate illuminated tables (Precision Vision, Bloomington, IL, USA), at a distance of 4 meters. The overall score takes into account the total number of letters read correctly.

4.3 Corneal confocal microscopy

All enrolled subjects underwent CCM, using Heidelberg Retina Tomography with the Rostock Cornea Module (HRTIII/RCM, Heidelberg Engineering, Germany). The HRTIII employs a 670 nm wavelength diode laser source and provides cross-sectional images of 400 × 400 μm, with a lateral resolution of 1 μm. For CCM imaging, a disposable sterile polymethylmethacrylate cap (TomoCap; Heidelberg Engineering) filled with hydroxypropyl methylcellulose 2.5% (GenTeal gel; Novartis Ophthalmics, East Hanover, New Jersey, USA) was placed on the objective lens of the Cornea Module, to improve optical coupling. After instillation of topical anesthesia, the Corneal Module was advanced manually until obtaining an appropriate cap contact with the corneal surface. Using the section mode of the CCM, layer per layer images of the central cornea full thickness were obtained. The three best focused non overlapping images of the sub-basal nerve plexus were selected for each of the examined eyes, and the average of the derived measures was used for further analyses. Firstly, a quantitative

automated image analysis software (ACCMetrics; University of Manchester, Manchester, UK, courtesy of Prof. Rayaz A. Malik) was used to calculate six parameters: Corneal Nerve Fiber Density (CNFD), the number of nerve fibers/mm^2; Corneal Nerve Branch Density (CNBD), the number of primary branch points on the main nerve fibers/mm^2; Corneal Nerve Fiber Length (CNFL), the total length of nerves mm/mm^2; Corneal Nerve Fiber Total Branch Density (CTBD), the total number of branch points/mm^2; Corneal Nerve Fiber Area (CNFA), the total nerve fiber area mm^2/mm^2; Corneal Nerve Fiber Width (CNFW), the average nerve fiber width mm/mm^2.[58–60] Two other parameters were obtained by a manual quantitative analysis performed by a blinded experienced operator on the best-quality image of the sub-basal nerve plexus: Number of Beadings (NBe) and Fiber Tortuosity (FT), according to previously reported methods.[61] NBe was defined as the number of hyperreflective points per unit of length (100 μm) of the best focused fiber, randomly chosen by the operator from all the nerve fibers seen in the corneal sub-basal nerve plexus image. Nerve beadings represent accumulation of mitochondria along the nerve, thus documenting the metabolic activity of corneal fibers sub-basal nerve plexus.[61,62] FT was classified using the grading system proposed by Oliveira-Soto which simultaneously considers the frequency and amplitude of changes in nerve fiber direction and provides a score ranging from 0 to 4, where 0 represents almost straight nerve fibers, 1 slightly tortuous fibers, 2 moderately tortuous fibers, 3 tortuous fibers with a quite severe amplitude of changes in fiber direction and 4 very tortuous nerve fibers, with abrupt and frequent changes in direction.[63] It is considered a morphologic marker of nerve degeneration and an attempt at fiber repair.[61,64]

4.4 Optical coherence tomography (OCT) and OCT angiography

All enrolled subjects underwent OCT and OCTA, using the Spectralis HRA + OCT2 platform (Heidelberg Engineering, Heidelberg, Germany), as previously described.[65–67] Both eyes of each subject were evaluated.

The following scans were obtained: a 20° x 20° volumetric macular map centered on the foveola, a circumpapillary ring scan with a diameter of 3.5 mm centered on the optic nerve head with a resolution of 100 ART, a 10° x 10° OCTA map centered on the foveola, a 20° x 20° OCTA map centered on the optic nerve head.

From the volumetric macular map the following parameters, automatically provided by the incorporated Spectralis software (Heyex Software, Heidelberg Eye Explorer; Heidelberg Engineering), were collected: the central subfield thickness (CST), represented by the mean retinal thickness of the central circular 1 mm centered on the foveola, and the total macular volume (MV), represented by the total retinal volume of the central circular 6 mm centered on the foveola.

From the circumpapillary ring scan the in-built software automatically provided the peripapillary retinal nerve fiber layer (pRNFL) thickness, expressed both as mean pRNFL (Global, G) and as mean sectorial pRNFL (Temporal, T; Temporal Superior, TS; Nasal Superior, NS; Nasal, N; Nasal Inferior, NI; Temporal Inferior, TI; Papillo-Macular Bundle, PMB).

With regard to OCT angiography, *en-face* images of the superficial vascular plexus (SVP), the intermediate capillary plexus (ICP), the deep capillary plexus (DCP), the choriocapillaris (CC) and the choroid (Ch) were obtained from the macular map and of the radial peripapillary capillary plexus (RPCP) from the optic nerve head map. All the images were automatically provided by the in-built segmentation algorithm, as previously described.[68] All images were reviewed to confirm consistent segmentation by the automated instrument software.

Quantitative analysis of the vascular plexuses in the OCTA *en-face* images was performed using the open-source, available ImageJ software (National Institutes of Health, Bethesda, MD, USA). For the SVP, ICP, DCP and RPCP, four parameters were analyzed: vessel area density (VAD), vessel length fraction (VLF), vessel diameter index (VDI) and fractal dimension (FD), as previously described.[69] Briefly, OCTA *en-face* images were automatically converted into binarized images to obtain VAD, dividing the

number of black pixels counted by the software in the binarized image by the total number of image pixels. After that, images were skeletonized (i.e. elaborated until a single pixel remains for each vessel segment) to obtain VLF, dividing the number of vessel pixels in the skeletonized image by the total number of image pixels. VDI was obtained by processing both the binarized and the skeletonized images to calculate the average vessel caliber. Finally, FD represents an index of complexity of the vessels' ramification, obtained on a skeletonized image by a specific count of differently sized squares containing a vessel fragment. With regard to the RPCP, the analysis was conducted after removing from the images the large vessels, according to a previously described method.[70] For the CC and Ch, the vascular/stromal ratio (V/S ratio) was obtained after elaboration of the images via ImageJ software, from the vessel density (V), defined as the proportion between the luminal area represented by white pixels and the total area, the stromal density (S), defined as 1 – V.[71]
All OCT and OCT angiography images were captured by an expert technician, while images' elaboration and analysis were conducted by a single masked operator.

4.5 Statistical analysis

Summary of study parameters was made according to usual methods provided by descriptive statistics: mean and standard deviation for quantitative variables; absolute and relative (percentage) frequencies for qualitative variables.
Demographic and descriptive parameters were compared among groups by ANOVA test or Chi-square test according to type of variable.
Analysis consisted in comparing Amyloidosis patients vs. Controls, and in comparisons among patients with different types of amyloidosis.
For quantitative parameters ANOVA for repeated measures model has been used. Measurement of parameter in both eyes of the same patient has been taken into account in all analyses. For qualitative parameters chi-square test has been used.

In case omnibus test resulted statistically significant, pairwise comparisons have been made by Tukey-Kramer post-hoc test for multiple comparisons and Chi-square test, if parameter was expressed as quantitative or qualitative variable respectively.
For all the analyses SAS® v.9.4 (SAS Institute, Cary, NC, USA) has been used. All tests have been interpreted as statistically significant if $P<0.05$.

5 RESULTS

5.1 Population

Thirty-five patients were enrolled, 32 males and 3 females. Seventeen patients were affected by ATTRwt amyloidosis, 9 patients by ATTRv amyloidosis (including one female) and two patients were pre-symptomatic carriers of the ATTR mutation. In addition, 7 patients with AL amyloidosis were enrolled (of which 2 were females). The mean age was 70.1 $\pm$ 11 years: 75 $\pm$ 7 for ATTRwt, 62 $\pm$ 8 for ATTRv and 73 $\pm$ 7 for AL amyloidosis patients. Four patients were also affected by diabetes mellitus (3 ATTRwt and 1 AL). Only three of these patients undergo regular eye examination. In the control group, 49 healthy subjects with a mean age of 66.2 $\pm$ 10.2 years were enrolled. The study and control groups did not differ as to mean age ($p=0.0964$). There was a significant difference in age among groups ($p=0.0044$), which was maintained only between ATTRwt and carriers in the single groups analysis ($p=0.0072$). With regard to the main systemic clinical manifestations, 17 patients presented clinical or instrumental signs of neuropathy, 30 of cardiomyopathy and 19 were affected by carpal tunnel syndrome, at the moment of the ocular examination. At the time of the ophthalmologic examination, five of nine ATTRv patients were in treatment with daily tafamidis (four at 20 mg and one at 61 mg), (as well as one with ATTRwt amyloidosis), four with patisiran. The other wtATTR patients were not under treatment for amyloidosis. All AL patients were under treatment with chemotherapy or immunotherapy associated with steroids.

Demographic and clinical characteristics of both groups are reported in Table 1 and 2.

Table 1. Clinical and demographic characteristics of enrolled subjects

	Amyloidosis Group	**Control Group**
Enrolled patients, n.	35	49
Age, mean ± SD, y	70.1 ± 11	66.2 ± 10.2
Sex, n. (%)		
Male	32 (91.2)	32 (64.4)
Female	3 (8.8)	17 (35.6)
Amyloidosis type, n. (%)		
ATTRwt	17 (48.6)	
ATTRv	9 (25.7)	
Pre-symptomatic carrier	2 (5.7)	
AL	7 (20)	
ATTRv mutation, n. (%)	9 (25.7)	
Val30Met	2 (22.2)	
Phe64Leu	2 (22.2)	
Glu62Lys	1 (11.1)	
Glu89Gln	1 (11.1)	
Val122Ile	1 (11.1)	
Ile68Leu	1 (11.1)	
Glu54Gln	1 (11.1)	
Diabetes, patients, n. (%)	4 (11.4)	0
Glaucoma, eyes, n. (%)	12 (17.1)	0
BCVA, mean ± SD ETDRS score	77.8 ±16.1	86.5 ± 1.7
Neuropathy, patients, n. (%)	17 (48.6)	
Cardiomyopathy, patients, n. (%)	30 (85.7)	
Carpal tunnel syndrome, patients, n. (%)	19 (54.3)	

N: number; y: years; SD: standard deviation; AL: light chain amyloidosis; ATTRv: hereditary transthyretin-related amyloidosis; ATTRwt: wild-type transthyretin-related amyloidosis; BCVA: best corrected visual acuity; ETDRS: Early treatment diabetic retinopathy research study.

The mean visual acuity of the entire study group was 77.8±16.1 ETDRS score, versus 86.5±1.7 for control group. Considering only the 17 ATTRwt patients, the visual acuity was 71.9 ± 21 ETDRS score. In both cases, visual

acuity was significantly reduced compared to the control group (visual acuity 86.5 ± 1.7, p=0.0001). In addition, the visual acuity of the ATTRwt group was more than 10 letters lower than other groups, however without reaching a statistical significance.

Table 2. Clinical and demographic characteristics of different amyloidosis groups

	ATTRwt	ATTRv	carrier	AL
Enrolled patients/eyes, n.	17/34	9/18	2/4	7/14
Age, mean±SD, y	75.1 ± 6.7	65.2 ± 13.4	50.5 ± 2.1	69.9 ± 9.7
Sex, n. (%)				
Male	17 (100)	8 (88.9)	2 (100)	5 (71.4)
Female	0	1 (11.1)	0	2 (28.6)
Diabetes, patients, n. (%)	4 (11.4)	0	0	1 (11.1)
Glaucoma, eyes, n. (%)	9 (26.5)	2 (11.1)	0	1 (7.1)
BCVA, mean±SD, ETDRS score	71.9 ± 21	82.8 ± 6.8	85.5 ± 3.1	83.5 ± 4.1
Cataract, eyes, n. (%)	17 (50)	6 (33.3)	0	2 (14.3)
IOL, eyes, n. (%)	13 (38.2)	2 (11.1)	0	4 (28.6)
RPE alterations, eyes, n. (%)	19 (55.9)	4 (22.2)	1 (25)	4 (28.6)
Vitreomacular interface alterations, eyes, n. (%)	4 (11.8)	3 (16.7)	0	0
Vitreous opacities, eyes, n. (%)	6 (17.7)	6 (33.3)	0	2 (14.3)
Neuropathy, patients, n. (%)	7 (41.2)	8 (88.9)	0	2 (28.6)
Cardiomyopathy, patients, n. (%)	17 (100)	6 (66.7)	0	7 (100)
Carpal tunnel syndrome, patients, n. (%)	12 (70.6)	6 (66.7)	0	1 (14.3)

N: number; y: years; SD: standard deviation; AL: light chain amyloidosis; ATTRv: hereditary transthyretin-related amyloidosis; ATTRwt: wild-type transthyretin-related amyloidosis; BCVA: best corrected visual acuity; ETDRS: Early treatment diabetic retinopathy research study; IOL: intraocular lens; CCM: corneal confocal microscopy.

Seventeen ATTRwt eyes presented with a clinically significant cataract, 8 of them requiring surgery; 13 ATTRwt eyes already underwent it. The two pre-symptomatic carriers of the ATTR gene mutation did not have cataract (Table 2). Mean intraocular pressure was 15 ± 4 mmHg, but 3 ATTRwt, 1 ATTRv and 1 AL patients were already on topical hypotonic treatment for glaucoma and two other ATTRwt patients were diagnosed with glaucoma by finding glaucoma-related field defects in the visual field and a corresponding reduction in peripapillary fibers at OCT. One of these patients presented with a picture of pseudoexfoliatio lentis in one eye, previously unknown. Only one ATTRv patient showed abnormal conjunctival vessels.

As for the alterations at the retinal level, in 28 eyes of 18 patients (13 ATTRwt, 2 ATTRv, 1 carrier and 2 AL), alterations in the retinal pigment epithelium, such as drusen or pigmentary alterations, were identified in the ophthalmoscopic examination and confirmed in the OCT examination. In three of these ATTRwt patients there was a picture of advanced maculopathy, two of which of first diagnosis, requiring a specific diagnostic-therapeutic path. Six patients (4 ATTRwt, 2 ATTRv and 1 AL) had a vitreoretinal interface syndrome with the presence of an epiretinal membrane and altered macular profile, one of these (AL) already surgically treated at another center, currently not in follow-up. Finally, vitreous opacities were identified at ophthalmoscopic examination in 7 patients (3 ATTRwt, 3 ATTRv and 1 AL), and 5 controls, but not clinically significant at the moment of the examination (Table 2). Therefore, no vitreoretinal surgical procedure was performed, considering the invasiveness of the procedure. One ATTRwt patient also showed signs of previous branch retinal vein occlusion.

In no patient deposits or further anomalies attributable to amyloidosis at the level of the iris were found. At the corneal level, epithelial and / or endothelial deposits were identified in 6 ATTRwt patients. These deposits were confirmed by the CCM, which also identified them in 10 other patients, (3 ATTRwt, 2 ATTRv, 3 AL, 1 pre-symptomatic carrier) (Table 4).

5.2 Corneal confocal microscopy results

The CCM examination found a significant reduction in the mean length of the sub-basal corneal plexus fibers (corneal nerve fiber length, CNFL, 9.7 ± 4.3 vs 12.4 ± 4.0, p = 0.0230), which was also confirmed after correction for glaucoma and diabetes (p=0.0270) (Table 3). Moreover, the examination showed tortuous stromal nerves in a greater number of amyloidosis eyes compared to controls (p=0.0094), as well as corneal deposits (30 vs 0 eyes, for amyloidosis and control eyes, respectively, p<0.0001). (Figure 6)

Table 3. Corneal confocal microscopy data in amyloidosis and control group.

Corneal Parameters, mean ± SD	**Amyloidosis Group**	**Control Group**	**p-value**	**p-value corrected for glaucoma and diabetes**
CNFD, n/mm²	13.2 ± 10	17.6 ± 8.4	0.0672	0.0893
CNBD, n/mm²	20 ± 20.9	25.3 ± 20.7	0.3480	0.3013
CNFL, mm/mm²	9.7 ± 4.3	12.4 ± 4	**0.0230**	**0.0270**
CTBD, n/mm²	36.1 ± 34	45.2 ± 26.8	0.2745	0.2015
CNFA, mm²/mm²	0.005 ± 0.003	0.006 ± 0.002	0.1523	0.1111
CNFW, mm/mm²	0.023 ± 0.003	0.023 ± 0.002	0.8894	0.7156
FT, range 0-4	2.3 ± 0.9	2.5 ± 0.8	0.4879	0.5603
NBe, n/100µm	8.8 ± 2.7	8.7 ± 1.4	0.9389	0.9259
Tortuous stromal nerves, eyes, n. (%)	19 (27.9)	2 (5.9)	**0.0094**	**0.0297**
Corneal deposits, eyes, n. (%)	30 (44.1)	0	**<0.0001**	**<0.0001**
Endothelial cells, n/mm²	2454.4 ± 509.5	2372.1 ± 217.3	0.4675	0.2276

SD: standard deviation; n: number; CNFD: corneal nerve fiber density; CNBD: corneal nerve branch density CNFL: corneal nerve fiber length; CTBD: corneal nerve total branch density; CNFA: corneal nerve fiber area; CNFW: corneal nerve fiber width; FT: fiber tortuosity; NBe: number of beadings; DC: dendritic cells; mm: millimeter; significant or borderline results (level of significance 0.05) in bold.

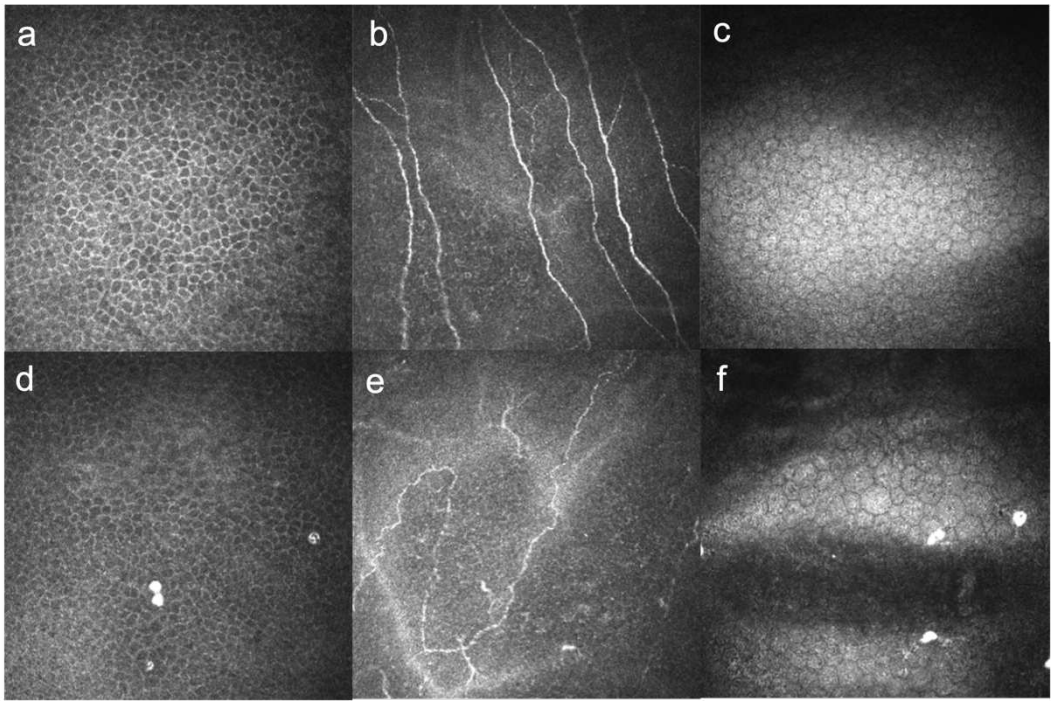

Figure 6: Images of the epithelium (a-b), the sub-basal nerve plexus (b-e) and the endothelium (c-f) captured with Heidelberg Retina Tomograph III Rostock Corneal Module (Heidelberg, Germany) from the central cornea of a healthy subject (a-c) and a ATTRwt subject (d-f). While the corneal nerve fibers of the healthy subject are mostly straight and continuous, those of the ATTRwt patient appear fragmented and more tortuous. Moreover, hyperreflective deposits may be observed both at the epithelium and the endothelium.

The comparison among groups (AL, ATTRwt, ATTRv, carriers) did not show significant differences, except for CNBD (p=0.0377) and tortuous stromal nerves (p=0.0052). When making a group to group comparison for these parameters, the only difference (borderline) was found between ATTRv and carriers (p=0.0696) for CNBD, and between AL vs ATTRwt and ATTRv vs ATTRwt (p=0.0330 and 0.0045, respectively). The results for multiple comparisons are reported in Tables 4 and 5.

No significant correlation with any major systemic manifestation was found for all the variables analyzed.

Table 4. Corneal confocal microscopy data in amyloidosis type groups.

	ATTRwt	ATTRv	carrier	AL	ANOVA p-value
CNFD, n/mm², mean ± SD	14.5 ± 9.9	11.3 ± 9.7	20.3 ± 6	10.3 ± 8	0.3596

CNBD, n/mm², mean ± SD	24.6 ± 23.6	10.9 ± 11.3	45.3 ± 12.9	12.1 ± 15.4	**0.0377**
CNFL, mm/mm², mean ± SD	9.7 ± 4.4	8 ±3.8	13 ± 3	8.4 ± 4	0.1963
CTBD, n/mm², mean ± SD	41.7 ± 38.9	26.2 ± 27.1	65.6 ± 25.8	25.4 ± 22.8	0.2153
CNFA, mm²/mm², mean ± SD	0.006 ± 0.003	0.004 ± 0.002	0.008 ± 0.002	0.004 ± 0.003	0.3147
CNFW, mm/mm², mean ± SD	0.023 ± 0.003	0.023 ± 0.003	0.023 ± 0.002	0.022 ± 0.003	0.6745
FT, range 0-4, mean ± SD	2.6 ± 0.9	1.8 ± 0.8	2.78 ± 0.5	2.2 ± 0.6	0.1052
NBe, n/100µm	8.8 ± 2.8	8.4 ± 2.5	9.8 ± 1.3	8.9 ± 3.3	0.9163
Tortuous stromal nerves, eyes, n. (%)	16 (47.1)	1 (6.3)	0	2 (14.3)	**0.0052**
Corneal deposits, eyes, n. (%)	18 (52.9)	4 (25)	2 (50)	6 (42.9)	0.3194
Endothelial cells, n/mm²	2442.7 ± 524.1	2516.8 ± 546.2	2429.3 ± 263.1	2418.4 ± 523.3	0.9764

SD: standard deviation; AL: light chain amyloidosis; ATTRv: hereditary transthyretin-related amyloidosis; ATTRwt: wild-type transthyretin-related amyloidosis; n: number; CNFD: corneal nerve fiber density; CNBD: corneal nerve branch density CNFL: corneal nerve fiber length; CTBD: corneal nerve total branch density; CNFA: corneal nerve fiber area; CNFW: corneal nerve fiber width; FT: fiber tortuosity; NBe: number of beadings; mm: millimeter; significant or borderline results (level of significance 0.05) in bold.

Table 5. Corneal confocal microscopy data in amyloidosis type groups: two groups comparison in multiple comparisons with p<0.05

p-value	AL vs ATTRvv	AL vs ATTRwt	AL vs carrier	ATTRv vs ATTRwt	ATTRv vs carrier	ATTRwt vs carrier
CNBD, n/mm²	0.9992	0.3651	0.0893	0.2553	0.0696	0.3759
Tortuous stromal nerves, eyes, n. (%)	0.4642	**0.0330**	0.4227	**0.0045**	0.6080	0.0714

AL: light chain amyloidosis; ATTRv: hereditary transthyretin-related amyloidosis; ATTRwt: wild-type transthyretin-related amyloidosis; n: number; CNBD: corneal nerve branch density; mm: millimeter.

5.3 Optical coherence tomography results

The OCT examination of the macular area showed a reduction in the mean macular volume (in the central macular area with a diameter of 6 mm), with an increase in the central subfield thickness (CST) in patients compared to

controls (p=0.0326 and p<0.0001, respectively) also after correction for diabetes and glaucoma (p=0.0003 and p=0.0180, respectively) (Table 6). These results have been influenced by the presence of an epiretinal membrane in 7 eyes (4 ATTRwt and 3 ATTRv), leading to a thickening involving the more central area of the macula, despite a generalized thinning of the whole macula, showed by the reduced volume (Table 6). In addition, a generalized reduction in the thickness of the peripapillary nerve fibers, both average and in each peripapillary sector (p <0.05), was identified, which was maintained in the superior temporal sector and in the average even after correction for glaucoma and diabetes (Table 6).

Table 6. Optical coherence tomography data in amyloidosis and control group.

Parameters, mean ± SD	**Amyloidosis Group**	**Control Group**	**p-value**	**p-value adjusted for glaucoma and diabetes**
Macular map				
CST, µm	297.3 ± 43.4	270 ± 17.2	**<0.0001**	**0.0003**
MV, mm^3	8.5 ± 0.7	8.8 ± 0.3	**0.0059**	**0.0180**
pRNFL				
Temporal	65.6 ± 13.2	71.1 ± 12.1	**0.0400**	0.1863
Temporal Superior	127.6 ± 26.7	145.3 ± 15.8	**<0.0001**	**0.0075**
Nasal Superior	102.8 ± 21.7	113.5 ± 21.3	**0.0243**	0.2458
Nasal	72.2 ± 17.3	79.8 ± 15.2	**0.0344**	0.3724
Nasal Inferior	110.1 ± 25.1	117.2 ±22.4	0.1745	0.6509
Temporal Inferior	129.7 ± 34.4	150.2 ± 17	**0.0002**	**0.0187**
Papillo-Macular Bundle	53.7 ±10.5	53.5 ± 7.2	0.8529	0.6215
Global	91.7 ± 16.7	103.3 ± 8.5	**<0.0001**	**0.0227**

SD: standard deviation; CST: central subfield thickness; µm: micrometer; MV: macular volume; µm: micrometer; mm: millimeter; pRNFL: peripapillary retinal nerve fiber layer; significant or borderline results (level of significance 0.05) in bold.

The comparison between groups (AL, ATTRwt, ATTRv, carriers) showed a significant difference among groups in the global peripapillary RNFL thickness and in the temporal and temporal inferior sectors (p=0.0413,

0.0205 and 0.0009, respectively), where the lowest thickness was found in the ATTRwt group (Table 7 and 8). No significant correlation with any major systemic manifestation was found for all the variables analyzed.

Table 7. Optical coherence tomography data in amyloidosis type groups.

	ATTRwt	ATTRv	carriers	AL	ANOVA p-value
Macular map parameters, mean ± SD					
CST, μm	305.6 ± 55.2	287.3 ± 24.2	292.5 ± 1.9	292.7 ± 36.5	0.6497
MV, mm^3	8.5 ± 0.8	8.5 ± 0.5	8.9 ± 0.0	8.5 ± 0.5	0.7861
pRNFL sector thickness, mean ± SD					
Temporal	61.6 ± 12.4	70.6 ± 8.6	86 ± 17.8	62.6 ± 11.4	**0.0205**
Temporal Superior	119.6 ± 26	134.6 ± 25.4	153.3 ± 5.4	128.7 ± 28.1	0.2061
Nasal Superior	98.5 ± 23.5	104.2 ± 13.3	107.8 ± 16	108.1 ± 26.2	0.7312
Nasal	69.8 ± 18.7	76.4 ± 12.1	67.5 ± 11.1	73.9 ± 20.4	0.7902
Nasal Inferior	107.3 ± 30.8	119.1 ± 21.4	104.5 ± 4.2	108.2 ± 18.3	0.6642
Temporal Inferior	110.1 ± 32.1	151.6 ± 16.9	178 ± 26.9	131.9 ± 26.8	**0.0009**
Papillo-Macular Bundle	53 ± 12.2	57.5 ± 7.7	62 ± 7.8	48.9 ± 8	0.1956
Global	83.9 ± 17.1	100.5 ± 9.3	106.3 ± 8.7	93.7 ± 16.7	**0.0413**

AL: light chain amyloidosis; ATTRv: hereditary transthyretin-related amyloidosis; ATTRwt: wild-type transthyretin-related amyloidosis; SD: standard deviation; n: number; CST: central subfield thickness; MV: macular volume; μm: micrometer; mm: millimeter; pRNFL: peripapillary retinal nerve fiber layer; significant or borderline results (level of significance 0.05) in bold.

Table 8. Optical coherence tomography data in amyloidosis type groups: two groups comparison in multiple comparisons with p<0.05

p-value	AL vs hATTR	AL vs wtATTR	AL vs carriers	hATTR vs wtATTR	hATTR vs carriers	wtATTR vs carriers
pRNFL sector						
Temporal	0.4797	0.9991	**0.0435**	0.2925	0.2775	0.0248
Temporal inferior	0.4325	0.2526	0.1028	**0.0059**	0.5249	**0.0053**
Global	0.7818	0.4567	0.6554	0.0719	0.9501	0.1661

AL: light chain amyloidosis; ATTRv: hereditary transthyretin-related amyloidosis; ATTRwt: wild-type transthyretin-related amyloidosis; pRNFL: peripapillary retinal nerve fiber layer; significant or borderline results (level of significance 0.05) in bold.

5.4 Optical coherence tomography angiography results

Finally, the study of retinal vascularization at OCT angiography showed a reduction in vascular density both at the level of the radial peripapillary capillary plexus (RPCP), located in the peripapillary nerve fiber layer, and at the level of the macular vascular plexuses, as well as at the level of the vascular component of the choriocapillary (even after correction for diabetes and glaucoma) (Table 9). (Figure 7)

Table 9. Optical coherence tomography angiography data in amyloidosis and control group.

Plexus	**Parameter** Mean ± SD	**Amyloidosis Group**	**Control Group**	**p-value**	**p-value adjusted for glaucoma and diabetes**
RPCP	VAD	0.431 ± 0.103	0.574 ± 0.051	**<0.0001**	**<0.0001**
	VLF	0.112 ± 0.028	0.148 ± 0.019	**<0.0001**	**<0.0001**
	VDI	3.919 ± 0.225	3.897 ± 0.220	0.6558	0.7227
	FD	1.550 ± 0.088	1.585 ± 0.027	**0.0094**	0.5881
SVP	VAD	0.282 ± 0.105	0.394 ± 0.062	**<0.0001**	**<0.0001**
	VLF	0.060 ± 0.021	0.087 ± 0.013	**<0.0001**	**<0.0001**
	VDI	4.645 ± 0.315	4.545 ± 0.243	0.1123	0.2058
	FD	1.409 ± 0.121	1.539 ± 0.054	**<0.0001**	**<0.0001**
ICP	VAD	0.112 ± 0.059	0.200 ± 0.057	**<0.0001**	**<0.0001**
	VLF	0.036 ± 0.017	0.061 ± 0.014	**<0.0001**	**<0.0001**
	VDI	2.927 ± 0.309	3.254 ± 0.230	**<0.0001**	**<0.0001**
	FD	1.255 ± 0.161	1.438 ± 0.077	**<0.0001**	**<0.0001**
DCP	VAD	0.148 ± 0.078	0.249 ± 0.081	**<0.0001**	**<0.0001**
	VLF	0.045 ± 0.021	0.071 ± 0.016	**<0.0001**	**<0.0001**
	VDI	3.119 ± 0.390	3.472 ± 0.536	**0.0002**	**0.0012**
	FD	1.312 ± 0.196	1.487 ± 0.078	**<0.0001**	**<0.0001**
CC	V/S ratio	0.558 ± 0.185	0.704 ± 0.135	**<0.0001**	**0.0004**
Ch	V/S ratio	0.607 ± 0.165	0.598 ± 0.134	0.8654	0.9469

SD: standard deviation; RPCP: radial peripapillary capillary plexus; SVP: superficial vascular plexus; ICP: intermediate capillary plexus; DCP: deep capillary plexus; CC: choriocapillaris; Ch: choroid; VAD: vessel area density; VLF: vessel length fraction; VDI: vessel diameter index; FD: fractal dimension; V/S ratio: vascular/stroma density ratio.

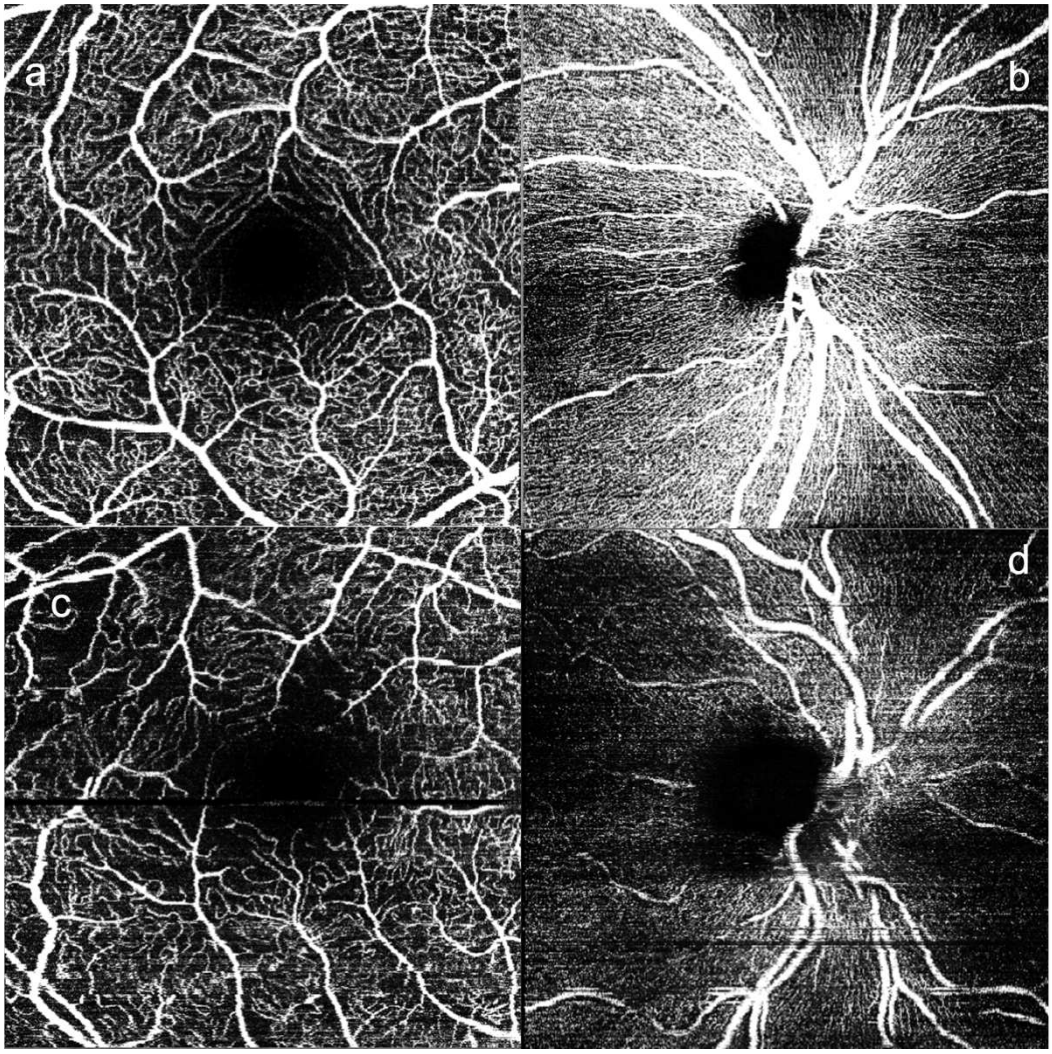

Figure 7: Images of the superficial vascular plexus (a-c) and the radial peripapillary capillary plexus (b-d) captured with Spectralis HRA + OCT2 platform (Heidelberg Engineering, Heidelberg, Germany) of a healthy subject (a-b) and a ATTRwt subject (c-d). While the plexi of the healthy subject are well represented, those of the ATTRwt patient show a reduction particularly in the density of the small vessels.

This reduction was particularly pronounced in ATTRwt and ATTRv patients compared to AL (and carriers), however without reaching consistent repeated statistically significant differences (Table 10 and 11). No significant correlation with any major systemic manifestation was found for all the variables analyzed.

Table 10. Optical coherence tomography angiography data in amyloidosis type groups.

Plexus	**Parameter,** Mean ± SD	**ATTRwt**	**ATTRv**	**carrier**	**AL**	**ANOVA p-value**

RPCP	VAD	0.4176 ± 0.0830	0.4066 ± 0.1388	0.5080 ± 0.0113	0.4700 ± 0.0851	0.4046
	VLF	0.1052 ± 0.0235	0.1065 ± 0.0387	0.1333 ± 0.0059	0.1250 ± 0.0138	0.2769
	VDI	4.0149 ± 0.1877	3.8021 ± 0.2754	3.8133 ± 0.1020	3.9170 ± 0.1627	0.0563
	FD	1.5419 ± 0.0661	1.5351 ± 0.1189	1.6105 ± 0.0124	1.5696 ± 0.0906	0.6028
SVP	VAD	0.2557 ± 0.0837	0.2847 ± 0.1216	0.4275 ± 0.0838	0.2801 ± 0.0885	0.1730
	VLF	0.0575 ± 0.0181	0.0593 ± 0.0248	0.0887 ± 0.0105	0.0574 ± 0.0168	0.2275
	VDI	4.4349 ± 0.1806	4.7766 ± 0.3351	4.7893 ± 0.3926	4.8479 ± 0.2299	**0.0055**
	FD	1.4004 ± 0.1034	1.3921 ± 0.1520	1.5437 ± 0.0359	1.4014 ± 0.0993	0.3582
ICP	VAD	0.0962 ± 0.0521	0.1130 ± 0.0645	0.1838 ± 0.0312	0.1171 ± 0.0562	0.2735
	VLF	0.0326 ± 0.0155	0.0360 ± 0.0187	0.0566 ± 0.0054	0.0381 ± 0.0155	0.3104
	VDI	2.8337 ± 0.2777	2.9490 ± 0.3476	3.2314 ± 0.2455	2.9835 ± 0.2646	0.3595
	FD	1.2217 ± 0.1592	1.2472 ± 0.1826	1.4223 ± 0.0265	1.2788 ± 0.1257	0.4074
DCP	VAD	0.1278 ± 0.0646	0.1475 ± 0.0918	0.2243 ± 0.0458	0.1640 ± 0.0759	0.3897
	VLF	0.0407 ± 0.0182	0.0445 ± 0.0253	0.0648 ± 0.0088	0.0489 ± 0.0189	0.4062
	VDI	3.0304 ± 0.3017	3.0787 ± 0.5129	3.4358 ± 0.2481	3.2652 ± 0.3089	0.3843
	FD	1.2924 ± 0.1613	1.2711 ± 0.2729	1.4660 ± 0.0369	1.3630 ± 0.1144	0.4750
CC	V/S ratio	0.4603 ± 0.1423	0.5901 ± 0.1682	0.8018 ± 0.2286	0.6331 ± 0.1575	**0.0400**
Ch	V/S ratio	0.5694 ± 0.1753	0.5772 ± 0.1074	0.6106 ± 0.2256	0.7436 ± 0.1483	0.1717

AL: light chain amyloidosis; ATTRv: hereditary transthyretin-related amyloidosis; ATTRwt: wild-type transthyretin-related amyloidosis; SD: standard deviation; RPCP: radial peripapillary capillary plexus; SVP: superficial vascular plexus; ICP: intermediate capillary plexus; DCP: deep capillary plexus; CC: choriocapillaris; Ch: choroid; VAD: vessel area density; VLF: vessel length fraction; VDI: vessel diameter index; FD: fractal dimension; V/S ratio: vascular/stroma density ratio; significant or borderline results (level of significance 0.05) in bold.

Table 11. Optical coherence tomography angiography data in amyloidosis type groups: two groups comparison in multiple comparisons with p≤0.05

p-value	AL vs ATTRv	AL vs ATTRwt	AL vs carrier	ATTRv vs ATTRwt	ATTRv vs carrier	ATTRwt vs carrier
RPCP VDI	0.6334	0.6412	0.8878	**0.0469**	0.9998	0.4121
SVP VDI	0.9910	**0.0243**	0.9932	**0.0131**	0.9998	0.2770
CC V/S ratio	0.9285	0.2397	0.6097	0.4174	0.3169	0.0556

AL: light chain amyloidosis; ATTRv: hereditary transthyretin-related amyloidosis; ATTRwt: wild-type transthyretin-related amyloidosis; pRNFL: peripapillary retinal nerve fiber layer; significant or borderline results (level of significance 0.05) in bold.

6 DISCUSSION

Several ocular manifestations have been described in ATTR amyloidosis, although mainly in case-series in ATTRv patients.[72–75] Ocular involvement has been reported in ATTRwt amyloidosis but only anecdotally.[76] Currently, the true prevalence of ATTRwt amyloidosis is unknown but it seems to be relatively high compared with the prevalence of ATTRv amyloidosis. In fact, autopsy studies showed ATTRwt fibrils in about 25% of the hearts of persons 80 years or older.[15,77] The greater awareness of the disease and the advancement in the diagnostic techniques have brought to an increase in the number of new diagnoses and an expansion of clinical spectrum.[54] Therefore, the definition of the possible clinical manifestations in these patients, also from an ophthalmological point of view, may significantly modify the management of the disease and their quality of life.

In our cohort of ATTRwt patients we found a high prevalence of ophthalmological alterations, involving both the anterior and the posterior segment of the eye and significantly modifying the visual function of the affected patients, also compared with patients affected by ATTRv and AL amyloidosis.

In particular, we found 17% of patients affected by glaucoma, with a particular high percentage in ATTRwt group (27%). Chronic open angle glaucoma has been already reported to be a main cause of irreversible visual loss in ATTRv patients. It seems to be due to the perivascular amyloid deposition in conjunctival and episcleral tissues and to the amyloid protein

released into the aqueous humor causing trabecular meshwork obstruction; these mechanisms may remain asymptomatic for months and years until the damage is irreversible, particularly in older patients, like the ATTRwt ones.[44] In fact, two new diagnoses of glaucoma (confirmed by pathological defects both at the peripapillary OCT and the visual field) were performed in our patients. This suggests the necessity of long-term monitoring and follow-up of IOP and evidence of deposits at the anterior segment in these patients. Moreover, the presence of the deposits causing ocular hypertension may reduce the efficacy of the conventional therapy, as already suggested for ATTRv amyloidosis. Therefore, a more aggressive treatment strategy should be always considered.[22,43,44,78]

With regard to OCT results, we found a reduction in the whole retinal thickness (MV), even after correction for diabetes and glaucoma and despite the presence of increase central thickness (CST) secondary to the presence of vitreomacular abnormalities. Therefore, a direct damage to the neuroepithelium seems to be due to the disease itself. Indeed, studies of immunochemistry showed an intense immunoreactivity particularly at the level of ganglion cells somata and axons of rats eyes.[21] Although we did not analyze each retinal layer thickness in the macula, we found a generalized reduction in the peripapillary retinal fiber layer, constituted by the axons of the ganglion cells, which may therefore be a direct consequence of the ganglion cells' impairment secondary to ATTR amyloidosis.

Moreover, TTR is a minor component of drusen, extracellular deposits of material found in the Bruch's membrane, which lay in conjunction with RPE and the choroid of the eye and are increased in age-related macular degeneration (AMD).[4] We found a very high prevalence of RPE alterations, including drusen, in the macula, with a prevalence of 55.9% and 22.2% in patients with ATTRwt and ATTRv amyloidosis, respectively, and even focal alterations in one eye of one carrier. The reported prevalence of the same alterations, is about 18% in age-matched general population.[79] Moreover, advanced maculopathy was detected in three of these ATTRwt

patients. For two of them the diagnosis was made during our examination and a specific therapeutic pathway was started. It is possible that in ATTRwt amyloidosis the accumulation of ATTR at the Bruch's membrane is enhanced, increasing the age-related degeneration of the complex constituted by RPE, Bruch's membrane and choriocapillaris, characteristic of AMD patients.

We also found a prevalence of 12% and 17% of alterations at the vitreomacular interface, mainly represented by a hyperreflective and thickened inner limiting membrane (ILM) at OCT. Although they may be found also in the general population, no control eye presented these alterations as well as AL patients. This finding might be related to the fact that the ATTR protein has high affinity for basement membranes, and the ILM is primarily composed of type IV collagen, which is also the major collagen of basement membranes.[23,80,81]

At present, OCT is surely the most diffusely used imaging modality for the diagnosis and follow-up of chorio-retinal diseases. It provides both qualitative (e.g. RPE and vitreomacular interface alterations) and quantitative data (CST, MV). However, the latter provide a general information on the retinal changes without distinguishing among the different retinal components, such as neurons, glia cell, vessels etc.[70] From this point of view CCM and OCT angiography provide more specific information on the different component of the cornea and on the retinal vessels, respectively. In particular, CCM allows the visualization of the single fibers of the sub-basal nerve plexus, *in vivo*. Moreover, differently from other studies, we used an automatic (and repeatable) method of quantification of CCM parameters, allowing a reliable evaluation of the nerve fibers.[45,58,82]

The neuroimaging study of the nerves has already shown its relevance in the diagnosis, or at least the diagnostic suspect, of ATTR-related polyneuropathy. Nerves at brachial plexus have proved to have a larger nerve cross-section area (CSA) at ultrasound in ATTRv patients when compared to pre-symptomatic carriers. Moreover, the ultrasound

abnormalities worsen in the follow-up both in patients and in carriers.[35,83,84] Moreover, keratoconjunctivitis sicca has been described in ATTRv amyloidosis, caused by the deposition of amyloid in the corneal layers, damaging epithelium and stroma and altering sensory innervation, with progressively reduced corneal sensitivity.[22,44] CCM in our population showed a reduction in sub-basal nerve fibers length and increased stromal nerve tortuosity, compared with control group. The studied population may be not comparable to the ATTRv population studied by nerve ultrasound, because of the different prevalence of mutations in our ATTRv patients and the different nerve structures studied, however CCM showed to be able to detect the nerve alterations in amyloidosis patients and its possible role as a valid diagnostic tool for early diagnosis and follow-up of nerve damage in these patients should be kept in mind.[83,84] In particular, we found a reduction in corneal nerve length (CNFL) in patients group compared to control. CNFL has already been shown to be the most reproducible and strong parameter for the detection of abnormalities of small fibers morphology in diabetes, also associated with different measures of neuropathy severity.[2] Moreover, Rousseau et al. proposed CNFL as a sensitive marker of denervation in ATTRv amyloidosis, correlating with the severity of both sensorimotor and autonomic neuropathies in ATTRv amyloidosis, as well as with clinical motor neuropathy and walking status and with lower limbs IntraEpidermal Nerve Fiber Density (IENFD). Therefore, we confirmed the relevance of CNFL not only in ATTRv but also in ATTRwt amyloidosis. We also found an increased number of tortuous stromal nerves, considered as suffering nerves, particularly in ATTRwt patients.[2] A high prevalence of carpal tunnel syndrome, spinal stenosis and polyneuropathy have been reported in ATTRwt patients, with evidence of sensory, sensorimotor and asymptomatic neuropathy at electrophysiology.[33,34] Moreover, an increased CSA at ultrasound has been shown also in ATTRwt patients as well as electrodiagnostic evidence of peripheral neuropathy in patients with no other causes of neuropathy confirming that peripheral nerve fibers involvement (large and small fibers

dysfunction), although less frequently, may occur in ATTRwt amyloidosis (chapter 2.4.2).[33] We confirmed the presence of these alterations in ATTRwt amyloidosis also at the level of the corneal nerve fiber in an objective a quantifiable way, using CCM.

OCT angiography allowed the identification of a diffuse reduction of all vascular parameters compared to controls both at the macular plexi and in the peripapillary plexus, without significant difference among groups. Signs of angiopathy, although rare, have been described in ATTRv patients using angiography with fluorescein and green indocyanine, requiring careful follow-up.[44,47] Moreover, retinal microangiopathy has been suggested to correlate to cerebral amyloid microangiopathy.[85] OCT angiography has shown to be able to detect the vascular impairment in a completely non-invasive way, even in the absence of clinically evident signs of vasculopathy at the fundus examination.

We found an impaired vascularization in all retinal plexi and choriocapillaris but not in the choroid, which is constituted by larger vessels than those in other plexi. It may be supposed that the damage secondary to amyloid deposition may influence first the small vessels, reducing blood flow. In vitro studies suggested that both ATTRwt and mutant ATTR regulate endothelial cell functions and oligomers formed during the process of amyloid fibril formation (chapter 2.3) play an important role in damaging the endothelial cells of blood vessels, process which seems to start before ATTR deposition.[23,73] Therefore, OCT angiography seems to be able to detect early chorioretinal vascular alteration.

Intraocular amyloid deposition also occurs in the anterior lens capsule, leading to early cataract.[44] We found a very high percentage of patients with cataract, requiring surgery, or patients who had already undergone it. Even if cataract is a cause of reversible visual loss and may be considered of secondary relevance comparted to the systemic manifestations, still it may create a significant discomfort in affected patients. Therefore, a specific follow-up should be performed also to assess this possible complication.

With regard to vitreous opacities, we found a prevalence of 14.3%, 17.7%, 33.3% and 10.2% in AL, ATTRv, ATTRwt patients and healthy controls, respectively, and in no subject the opacities were clinically significant, in term of visual function. No pseudopodia lentis, glass wool vitreous, and retinal perivascular amyloid deposits were detected, therefore the opacities detected in our cohort may not be surely correlated to amyloid deposits.[86] Although vitreous opacities are described as a frequent and disabling manifestation in ATTRv amyloidosis in different papers, in our group of ATTRwt patients the prevalence of clinically relevant vitreous opacities was not significant. However, literature data are very variable even in the ATTRv cohorts, also depending on the prevalence of different mutations, and in a recent series of 18 ATTRv eyes no vitreous opacity was detected.[40,45,78] Moreover, they are described as a late manifestation and the definition of opacities is strictly dependent on the examining clinician, making this finding less reliable compared to the other ophthalmologic data reported.[87]

We also found only one patient (ATTRv) in the whole cohort with significant abnormal conjunctival vessels, frequently described in other series of ATTRv amyloidosis, even if with a high variability of results among studies and even among different populations within the same study.[44,74,87] The absence of such abnormalities in our ATTRwt patients may be due to the different conformation and behavior of ATTR fibrils in wt and ATTRv amyloidosis (2.4.2). With regard to ATTRv amyloidosis, all our patients were under treatment and abnormal conjunctival vessels have been supposed to be derived from the circulating mutated protein. It is therefore possible that therapy may have influenced the development of this conjunctival sign.[22,31,44]

Ocular manifestations of AL patients most frequently include involvement of the temporal artery, conjunctiva, extraocular muscles, trabecular meshwork, and cranial nerves. Moreover, AL patients may show occupying-space masses invading these ocular tissues, which are less frequently described in ATTR patients. In our series, although limited in number, we found a reduction in nerve fibers length and a general reduction in macular volume

and in the peripapillary nerve fiber layer, in line with other patients, even in the AL group, confirming the systemic amyloid neuropathy already reported in these patients. We did not find significant restriction in ocular movements or periorbital lesions, however all our patients were already under treatment.[8,18]

We did not find any correlation among OCT, OCT angiography and CCM and systemic amyloidosis-related manifestations, as already previously reported.[22] However, we did not analyze the correlation with single parameters of systemic polyneuropathy and/or cardiomyopathy, but with the presence of these phenotypes as diagnosed on the basis of a series of examinations. Further studies might correlate the ocular damage biomarkers to different parameters of systemic involvement (such as CSA at ultrasound or electrochemical skin conductance).

With the advent of the new therapeutic options for ATTR amyloidosis, good results have been obtained in reducing disease progression and obtain longer survival. However, liver transplant has been confirmed to not influence the course of eye and central nervous system manifestations, and even higher concentration of ATTR have been found in aqueous humor in a patient who underwent liver transplantation.[88] Moreover, most of the currently approved treatments are not able to cross the blood-brain barrier. Therefore, the clinical manifestations involving the central nervous system and the eye may become the most prevalent ones in the near future.[36,54,57]

Tafamidis has been suggested to be the only approved drug that is able to cross, in minimal part, the blood-brain and blood-eye barriers, limiting the effects on the central nervous system and the eye.[36,57] However, more data are necessary to understand if and how this and new drugs may cross the blood-brain and blood-eye barriers and inhibit local fibrillogenesis.[89]

Since no plasma or urinary biomarker is available for the diagnosis of ATTR amyloidosis, recently, the development of specific screening programs for the early identification of ATTR, particularly ATTR amyloidosis, has been proposed.[15] The combination of different clinical features, such as the

presence of nerve fibers alterations, anterior segment (at CCM) and posterior segment (at OCT) deposits, associated with other proposed early manifestations of the disease, such as carpal tunnel syndrome, may anticipate the suspicious of ATTR amyloidosis, particularly ATTRwt amyloidosis, and lead to the correct diagnosis and management. This may be of primary importance also in pre-symptomatic carriers, where the detection of the first signs of the disease may allow a timely treatment.

It is important to not underestimate the relevance of a thorough and regular ophthalmological follow-up in all ATTR patients, not only from an individual clinical point of view, but also to better understand the timing of the ophthalmological manifestations with respect to the systemic ones and the type of ATTR amyloidosis (wt/v/different mutations).

One of the main confounding factors in our population was the old age, particularly in ATTRwt patients, where a high prevalence of alterations usually due to degeneration and ageing were found. However, as previously suggested, it is possible that some alterations are correlated more to age than to amyloidosis, but it is unlikely that they are not correlated at all, since amyloidosis can potentiate the effect of any other degenerative and vascular process.[90]

The main limitations of our study were its cross-sectional design and the limited sample size. However, this study represents, at least for ATTRwt amyloidosis, one of the largest cohorts so far described, particularly from an ophthalmological point view. We analyzed both eyes of all subjects, however we did consider the possible interdependence of the results obtained from the same subject and all analyses were performed for repeated measures, as reported in the methods section, to limit bias on the results.

Finally, the relationship between the amyloid deposition and the clinical manifestations found in this study has not been confirmed by immunohistochemical colorations (Congo red) and no typing of amyloid proteins has been performed. However, the presence of TTR amyloid in the different tissues of the eye has already been proven.[39,86,88] Therefore,

considering the invasiveness of the procedure in the eye and the inaccessibility of some involved ocular tissues *in vivo*, most studies on ATTR amyloidosis do not perform a specific histology of ocular manifestations.[28,31]

7 CONCLUSIONS

In conclusion, ATTRwt amyloidosis is a systemic disease that could potentially lead to severe ocular involvement with significant consequences in term of visual acuity and quality of life, also compared to more studied amyloidosis forms, such as ATTRv and AL amyloidosis. Therefore, in ATTRwt patients a multidisciplinary management with regular ophthalmological assessments should be recommended from the moment of diagnosis in order to identify, adequately follow and eventually treat the alterations that tend to appear over time in different ocular structures. Moreover, a higher awareness of the ophthalmological alterations which characterize ATTR amyloidosis may contribute to precociously identify patients at risk of systemic complications, and to allow a timely treatment.

8 BIBLIOGRAPHY

1. Midena E, Frizziero L, Parrozzani R. Eye Signs of Wilson Disease: On and Beyond the Surface. In: Clinical and Translational Perspectives on WILSON DISEASE. Academic Press; 2019. p. 227–35.
2. Cosmo E, Midena G, Frizziero L, et al. Corneal Confocal Microscopy as a Quantitative Imaging Biomarker of Diabetic Peripheral Neuropathy: A Review. J Clin Med. 2022;11:5130.
3. Galloway NR, Amoaku WMK, Galloway PH, et al. (2022). Basic Anatomy and Physiology of the Eye. In: Common Eye Diseases and their Management. Springer, Cham.
4. Buxbaum JN, Reixach N. Transthyretin: the servant of many masters. Cell Mol Life Sci. 2009;66:3095–101.
5. Campbell JP, Zhang M, Hwang TS, et al. Detailed Vascular Anatomy of the Human Retina by Projection-Resolved Optical Coherence Tomography Angiography. Sci Rep. 2017;7:42201.
6. Midena E, Marchione G, Di Giorgio S, et al. Ultra-wide-field fundus photography compared to ophthalmoscopy in diagnosing and classifying major retinal diseases. Sci Rep. 2022;12:19287.
7. Spaide RF, Fujimoto JG, Waheed NK, et al. Optical coherence tomography angiography. Prog Retin Eye Res. 2018;64:1–55.
8. Wechalekar AD, Gillmore JD, Hawkins PN. Systemic amyloidosis. Lancet (London, England). 2016;387:2641–54.
9. Picken MM. The Pathology of Amyloidosis in Classification: A Review. Acta Haematol. 2020;143:322–34.
10. Westermark P, Benson MD, Buxbaum JN, et al. A primer of amyloid nomenclature. Amyloid. 2007;14:179–83.
11. Buxbaum JN, Dispenzieri A, Eisenberg DS, et al. Amyloid nomenclature 2022: update, novel proteins, and recommendations by the International Society of Amyloidosis (ISA) Nomenclature Committee. Amyloid. 2022;29:213–9.

12. Briani C, Cavallaro T, Ferrari S, et al. Sporadic transthyretin amyloidosis with a novel TTR gene mutation misdiagnosed as primary amyloidosis. J Neurol. 2012;259:2226–8.
13. Massie R. Peripheral Neuropathy in Wild-Type Amyloidosis: The More You Look, the More You Will Find. Can J Neurol Sci. 2021;48:597–8.
14. Russo M, Obici L, Bartolomei I, et al. ATTRv amyloidosis Italian Registry: clinical and epidemiological data. Amyloid. 2020;27:259–65.
15. Maurer MS, Bokhari S, Damy T, et al. Expert Consensus Recommendations for the Suspicion and Diagnosis of Transthyretin Cardiac Amyloidosis. Circ Heart Fail. 2019;12:e006075.
16. Visentin A, Briani C, Imbergamo S, et al. Idelalisib plus rituximab is effective in systemic AL amyloidosis secondary to chronic lymphocytic leukaemia. Hematol Oncol. 2018;36:366–9.
17. Dammacco R, Merlini G, Lisch W, et al. Amyloidosis and Ocular Involvement: an Overview. Semin Ophthalmol. 2020;35:7–26.
18. Reynolds MM, Veverka KK, Gertz MA, et al. OCULAR MANIFESTATIONS OF SYSTEMIC AMYLOIDOSIS. Retina. 2018;38:1371–6.
19. Tong JY, Juniat V, McKelvie PA, et al. Clinical and Radiological Features of Intramuscular Orbital Amyloidosis: A Case Series and Literature Review. Ophthal Plast Reconstr Surg. 2022;38:234–41.
20. Adams D, Suhr OB, Hund E, et al. First European consensus for diagnosis, management, and treatment of transthyretin familial amyloid polyneuropathy. Curr Opin Neurol. 2016;29 Suppl 1:S14–26.
21. Dwork AJ, Cavallaro T, Martone RL, et al. Distribution of transthyretin in the rat eye. Invest Ophthalmol Vis Sci. 1990 Mar 1;31:489-96.
22. Martins AC, Rosa AM, Costa E, et al. Ocular Manifestations and Therapeutic Options in Patients with Familial Amyloid

Polyneuropathy: A Systematic Review. Biomed Res Int. 2015;2015:282405.

23. Koike H, Katsuno M. Transthyretin Amyloidosis: Update on the Clinical Spectrum, Pathogenesis, and Disease-Modifying Therapies. Neurol Ther. 2020;9:317–33.
24. Salvalaggio A, Cacciavillani M, Tiengo C, et al. Multimodal evaluation of carpal tunnel syndrome in a pre-symptomatic TTR mutation carrier. J Neurol Sci. 2023;120596.
25. Briani C, Adami F, Cavallaro T, et al. Axonal neuropathy due to myelin protein zero mutation misdiagnosed as amyloid neuropathy. Muscle Nerve. 2008;38:921–3.
26. Fortuna A, Salvalaggio A, Cipriani A, et al. Autonomic dysfunction as first presentation of Glu54Gln transthyretin amyloidosis. J Neurol Sci. 2022;437:120264.
27. Cappellari M, Cavallaro T, Ferrarini M, et al. Variable presentations of TTR-related familial amyloid polyneuropathy in seventeen patients. J Peripher Nerv Syst. 2011;16:119–29.
28. Ruiz-Medrano J, Puertas M, Almazán-Alonso E, et al. OPHTHALMOLOGIC INVOLVEMENT IN PATIENTS WITH HEREDITARY TRANSTHYRETIN AMYLOIDOSIS. Retina. 2023;43:49-56.
29. Adams D, Koike H, Slama M, Coelho T. Hereditary transthyretin amyloidosis: a model of medical progress for a fatal disease. Nat Rev Neurol. 2019;15:387–404.
30. Tozza S, Severi D, Spina E, et al. The neuropathy in hereditary transthyretin amyloidosis: A narrative review. J Peripher Nerv Syst. 2021;26:155–9.
31. aus dem Siepen F, Hein S, Prestel S, et al. Carpal tunnel syndrome and spinal canal stenosis: harbingers of transthyretin amyloid cardiomyopathy? Clin Res Cardiol. 2019;108:1324–30.
32. González-López E, Gallego-Delgado M, Guzzo-Merello G, et al. Wild-type transthyretin amyloidosis as a cause of heart failure with

preserved ejection fraction. Eur Heart J. 2015;36:2585–94.
33. Campagnolo M, Cacciavillani M, Cipriani A, et al. Peripheral nerve involvement in wild-type transthyretin amyloidosis. Neurol Sci. 2023;44:351–4.
34. Russell A, Hahn C, Chhibber S, et al. Utility of Neuropathy Screening for Wild-Type Transthyretin Amyloidosis Patients. Can J Neurol Sci. 2021;48:607–15.
35. Salvalaggio A, Coraci D, Obici L, et al. Progressive brachial plexus enlargement in hereditary transthyretin amyloidosis. J Neurol. 2022;269:1905–12.
36. Buxbaum JN, Brannagan T, Buades-Reinés J, et al. Transthyretin deposition in the eye in the era of effective therapy for hereditary ATTRV30M amyloidosis. Amyloid. 2019;26:10–4.
37. Pino RM. Restriction of exogenous transthyretin (prealbumin) by the endothelium of the rat choriocapillaris. Am J Anat. 1986;177:63–70.
38. Iakovleva I, Hall M, Oelker M, et al. Structural basis for transthyretin amyloid formation in vitreous body of the eye. Nat Commun. 2021;12:7141.
39. Haraoka K, Ando Y, Ando E, et al. Amyloid deposition in ocular tissues of patients with familial amyloidotic polyneuropathy (FAP). Amyloid. 2002;9:183–9.
40. Leung KCP, Ko TCS. Ocular manifestations in hereditary transthyretin Gly67Glu amyloidosis. Amyloid. 2019;26:171–2.
41. Brodie FL, Jaffe GJ. Choroidal Neovascularization in Familial Transthyretin Amyloidosis. Retina. 2021;41:e44–5.
42. Thiagasorupan P, Barreau E, Gendron G, et al. Specific postoperative complications of vitrectomy in hereditary transthyretin amyloidosis. Eur J Ophthalmol. 2021;32:1149–56.
43. Beirão JM, Moreira LM, et al. Aqueous humor erythropoietin levels in open-angle glaucoma patients with and without TTR V30M familial amyloid polyneuropathy. Mol Vis. 2014;20:970–6.
44. Minnella AM, Rissotto R, Antoniazzi E, et al. Ocular Involvement in

Hereditary Amyloidosis. Genes (Basel). 2021;12:955.
45. Minnella AM, Rissotto R, Maceroni M, et al. Ocular Involvement in Hereditary Transthyretin Amyloidosis: A Case Series Describing Novel Potential Biomarkers. Genes (Basel). 2021;12:927.
46. Rousseau A, Cauquil C, Dupas B, et al. Potential Role of In Vivo Confocal Microscopy for Imaging Corneal Nerves in Transthyretin Familial Amyloid Polyneuropathy. JAMA Ophthalmol. 2016;134:983–9.
47. Kawaji T, Ando Y, Nakamura M, et al. Ocular amyloid angiopathy associated with familial amyloidotic polyneuropathy caused by amyloidogenic transthyretin Y114C. Ophthalmology. 2005;112:2212.
48. Kojima A, Ohno-Matsui K, Mitsuhashi T, et al. Choroidal vascular lesions identified by ICG angiography in a case of familial amyloidotic polyneuropathy. Jpn J Ophthalmol. 2003;47:97–101.
49. Meira AT, Sato MT, Shiokawa N, et al. Retinal amyloid angiopathy. Arq Neuropsiquiatr. 2022;80:335–6.
50. Falls HF, Jackson J, Carey JH, et al. Ocular manifestations of hereditary primary systemic amyloidosis. AMA Arch Ophthalmol. 1955;54:660–4.
51. Hamann S, Jensen PK, Fledelius HC. Bilateral optic neuropathy in a patient with familial amyloidotic polyneuropathy. BMJ Case Rep. 2013;2013:bcr2013200445.
52. Beirão JM, Malheiro J, Lemos C, et al. Impact of liver transplantation on the natural history of oculopathy in Portuguese patients with transthyretin (V30M) amyloidosis. Amyloid. 2015;22:31–5.
53. European Medicines Agency. (2011, 18 Nov, updated 2023, 24 Feb) *VYNDAQEL ANNEX I SUMMARY OF PRODUCT CHARACTERISTICS.* Available at https://www.ema.europa.eu/en/documents/product-information/vyndaqel-epar-product-information_en.pdf [Accessed on 2023 March 12]

54. Dohrn MF, Medina J, Olaciregui Dague KR, et al. Are we creating a new phenotype? Physiological barriers and ethical considerations in the treatment of hereditary transthyretin-amyloidosis. Neurol Res Pract. 2021;3:57.
55. Adams D, Tournev IL, Taylor MS, et al. Efficacy and safety of vutrisiran for patients with hereditary transthyretin-mediated amyloidosis with polyneuropathy: a randomized clinical trial. Amyloid. 2023;30:1-9.
56. European Medicines Agency. (2022, 12 Oct, updated 2023, 10 Jan) *AMVUTTRA ANNEX I SUMMARY OF PRODUCT CHARACTERISTICS.* Available at https://www.ema.europa.eu/en/documents/product-information/amvuttra-epar-product-information_en.pdf [Accessed on 2023 May 10]
57. Monteiro C, Martins da Silva A, Ferreira N, et al. Cerebrospinal fluid and vitreous body exposure to orally administered tafamidis in hereditary ATTRV30M (p.TTRV50M) amyloidosis patients. Amyloid. 2018;25:120–8.
58. Dabbah MA, Graham J, Petropoulos IN, et al. Automatic analysis of diabetic peripheral neuropathy using multi-scale quantitative morphology of nerve fibres in corneal confocal microscopy imaging. Med Image Anal. 2011;15:738-47.
59. Dabbah MA, Graham J, Petropoulos I, et al. Dual-Model Automatic Detection of Nerve-Fibres in Corneal Confocal Microscopy Images. Med Image Comput Comput Assist Interv. 2010;13:300–7.
60. Chen X, Graham J, Dabbah MA, et al. An Automatic Tool for Quantification of Nerve Fibres in Corneal Confocal Microscopy Images. IEEE Trans Biomed Eng. 2017;64:786–94.
61. Midena E, Brugin E, Ghirlando A, et al. Corneal Diabetic Neuropathy: A Confocal Microscopy Study. 2006;22:1047–52.
62. Gambato C, Longhin E, Catania AG, et al. Aging and corneal layers: an in vivo corneal confocal microscopy study. Graefes Arch Clin Exp

Ophthalmol. 2015;253:267-75.
63. Oliveira-Soto L, Efron N. Morphology of corneal nerves using confocal microscopy. Cornea. 2001;20:374–84.
64. Kallinikos P, Berhanu M, O'Donnell C, et al. Corneal nerve tortuosity in diabetic patients with neuropathy. Invest Ophthalmol Vis Sci. 2004;45:418-22.
65. Frizziero L, Midena G, Longhin E, et al. Early Retinal Changes by OCT Angiography and Multifocal Electroretinography in Diabetes. J Clin Med. 2020;9:3514.
66. Midena E, Torresin T, Longhin E, et al. Early Microvascular and Oscillatory Potentials Changes in Human Diabetic Retina: Amacrine Cells and the Intraretinal Neurovascular Crosstalk. J Clin Med. 2021;10:4035.
67. Pilotto E, Nacci EB, De Mojà G, et al. Structural and microvascular changes of the peripapillary retinal nerve fiber layer in Von Hippel-Lindau disease: an OCT and OCT angiography study. Sci Rep. 2021;11:25.
68. Pilotto E, Torresin T, Leonardi F, et al. Retinal Microvascular and Neuronal Changes Are Also Present, Even If Differently, in Adolescents with Type 1 Diabetes without Clinical Diabetic Retinopathy. J Clin Med. 2022;11:3982.
69. Parrozzani R, Leonardi F, Frizziero L, et al. Retinal Vascular and Neural Remodeling Secondary to Optic Nerve Axonal Degeneration: A Study Using OCT Angiography. Ophthalmol Retin. 2018;2:827–35.
70. Frizziero L, Parrozzani R, Londei D, et al. Quantification of vascular and neuronal changes in the peripapillary retinal area secondary to diabetic retinopathy. Br J Ophthalmol. 2021;105:1577-1583.
71. Cicinelli MV, Rabiolo A, Marchese A, et al. Choroid morphometric analysis in non-neovascular age-related macular degeneration by means of optical coherence tomography angiography. Br J Ophthalmol. 2017;101:1193–200.

72. Sandgren O. Ocular amyloidosis, with special reference to the hereditary forms with vitreous involvement. Surv Ophthalmol. 1995;40:173–96.
73. Rousseau A, Terrada C, Touhami S, et al. Angiographic Signatures of the Predominant Form of Familial Transthyretin Amyloidosis (Val30Met Mutation). Am J Ophthalmol. 2018;192:169–77.
74. Reynolds MM, Veverka KK, Gertz MA, et al. Ocular Manifestations of Familial Transthyretin Amyloidosis. Am J Ophthalmol. 2017;183:156–62.
75. Latasiewicz M, Sala-Puigdollers A, Gonzalez-Ventosa A, Milla E, Adan Civera A. Multimodal retinal imaging of familial amyloid polyneuropathy. Ophthalmic Genet. 2019;40:407–20.
76. Barouch FC, Benson MD, Mukai S. Isolated vitreoretinal amyloidosis in the absence of transthyretin mutations. Arch Ophthalmol (Chicago, Ill 1960). 2004;122:123–5.
77. Vergaro G, Solal AC, Emdin M. Wild type transthyretin amyloidosis: Don't miss diagnosis! Int J Cardiol. 2020;312:96–7.
78. Liu T, Zhang B, Jin X, et al. Ophthalmic manifestations in a Chinese family with familial amyloid polyneuropathy due to a TTR Gly83Arg mutation. Eye (Lond). 2014;28:26–33.
79. Rein DB, Wittenborn JS, Burke-Conte Z, et al. Prevalence of Age-Related Macular Degeneration in the US in 2019. JAMA Ophthalmol. 2022;140:1202–8.
80. Levison AL, Kaiser PK. Vitreomacular interface diseases: Diagnosis and management. Taiwan J Ophthalmol. 2014;4:63–8.
81. Gatseva A, Sin YY, Brezzo G, Van Agtmael T. Basement membrane collagens and disease mechanisms. Essays Biochem. 2019;63:297.
82. Petropoulos IN, Manzoor T, Morgan P, et al. Repeatability of in vivo corneal confocal microscopy to quantify corneal nerve morphology. Cornea. 2013;32:e83-9.
83. Salvalaggio A, Coraci D, Cacciavillani M, et al. Nerve ultrasonography features in hereditary transthyretin amyloidosis with

V30M mutation and polyneuropathy. Neurol Sci. 2021;42:2547–8.
84. Salvalaggio A, Coraci D, Cacciavillani M, et al. Nerve ultrasound in hereditary transthyretin amyloidosis: red flags and possible progression biomarkers. J Neurol. 2021;268:189–98.
85. Alber J, Arthur E, Goldfarb D, et al. The relationship between cerebral and retinal microbleeds in cerebral amyloid angiopathy (CAA): A pilot study. J Neurol Sci. 2021;423:117383.
86. Venkatesh P, Selvan H, Singh SB, et al. Vitreous Amyloidosis: Ocular, Systemic, and Genetic Insights. Ophthalmology. 2017;124:1014–22.
87. Beiraõ JM, Malheiro J, Lemos C, et al. Ophthalmological manifestations in hereditary transthyretin (ATTR V30M) carriers: A review of 513 cases. Amyloid. 2015;22:117–22.
88. Haraoka K, Ando Y, Ando E, et al. Presence of variant transthyretin in aqueous humor of a patient with familial amyloidotic polyneuropathy after liver transplantation. Amyloid. 2002;9:247–51.
89. Clinical Trials.gov. (2018, 19 July) Short-term Effects of TOLCAPONE on Transthyretin Stability in Subjects With Leptomeningeal TTR Amyloidosis (ATTR) - Available at https://clinicaltrials.gov/ct2/show/NCT03591757 [Accessed on 2023 March 12].
90. Reynolds MM, Veverka KK, Gertz MA, et al. Ocular Manifestations of Familial Transthyretin Amyloidosis. Am J Ophthalmol. 2017 Nov;183:156-162.